Study of Two-Photon Excited Fluorescence Microscopy for Spectroscopic Studies of Tissue

Diploma Paper
by
Mårten Öbrink

Lund Reports on Atomic Physics, LRAP-178
February, 1995

1. Abstract

Autofluorescence from different samples have been studied spectroscopically using a two-photon excited fluorescence microscopic technique. Untreated rat-liver tissue and liver from rats injected with ALA, as well as paper samples, have been examined. The optics of the microscope have been optimised through investigation of the properties of different microscope lenses when used in two-photon excited fluorescence microscopy. The pulse broadening in a Nikon CF N Plan Apochromat objective has been measured.
Disturbances in form of unwanted background peaks in the recorded spectra, making Photosensitiser-detection impossible, have been obliterated.
To be able to estimate the extension of the photobleaching in the sample, in the vicinity of the focus for a two-photon excited process, and hence predict the spatial resolution, a measurement of the size of the focal-point has been made. An estimation of the focus volume is presented.

Contents

2. Introduction

At the Division of Atomic Physics and the Lund University Medical Laser Centre, a non-intrusive method to detect and treat small malignant tumours using laser spectroscopic techniques and photodynamic therapy (PDT) has been developed. The project started in 1982 and since some time, a method for treating skin cancer is being used at Lund University Hospital [1]. These medical laser projects have branched of a multitude of different research-projects for detection and treatment of several different types of cancer lesions. The two-photon excited fluorescence scanning microscopy project in which this diploma paper takes part, is one of these projects.

2.1 Medical principles

2.1.1 Tumour selectivity

To be able to spectroscopically distinguish malignant tissue from normal surrounding tissue in fluorescence tissue diagnostics, a tumour-selective agent is usually administrated to the patient. Examples of such tumour-selective agents are δ-amino levulinic acid (ALA)-induced Protoporphyrin IX (PpIX), and a haematoporphyrin derivative (Photofrin). These drugs are photodynamically active, meaning that they catalyse photochemical reactions and thereby sensitise tissue to light. They can be used for photodynamic therapy, PDT, of malignant tumours. (Such photodynamically active substances are in this paper generally referred to as photosensitisers).

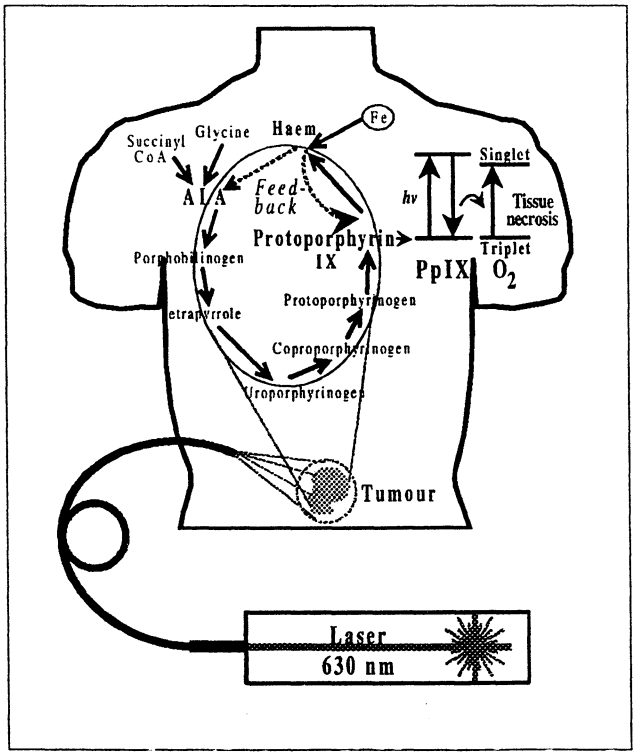

Fig. 2.1. The Haem-cycle, in which photosensitive PpIX is produced. The detected tumour is finally treated through illumination with laser light. From Ref.[1].

Some time after ALA administration, the human body has transformed ALA into PpIX. This process takes part in the mitochondria of the cell. The photosensitisers have good tumour-selective properties meaning that they accumulate in tumour tissue. After a certain period of time (from 3 hours up to 1 day) the concentration of photosensitisers in the tumours is much higher than in normal tissue since malignant tumours will retain the photosensitiser longer than non-malignant tissue. For most tumour types the difference in concentration is two to five times.

2.1.2 Detection

The use of a tumour-selective agent that can be used as a fluorescence marker is essential to be able to demarcate malignancies. The skin is illuminated with light from a nitrogen-laser pumped dye-laser, λ = 405 nm, through an optical fiber. A spectrum of the fluorescence light is recorded and from the spectral information it is possible to decide whether the tissue is malignant or not. The fluorescence-spectrum from a tumour differs a lot from that of normal tissue, as can be seen in *fig. 2.2.*
Healthy tissue (without photosensitiser) normally has its fluorescence-maximum around 500 nm, while the photosensitiser used have a major fluorescence-peak at 630-635 nm and a minor at 695-700 nm. Through calculating the ratio between the intensity at 630-635 and 500 nm, a value corresponding to the relative concentration of photosensitiser in the tissue is obtained. A tumour can in this way be demarcated from healthy tissue.

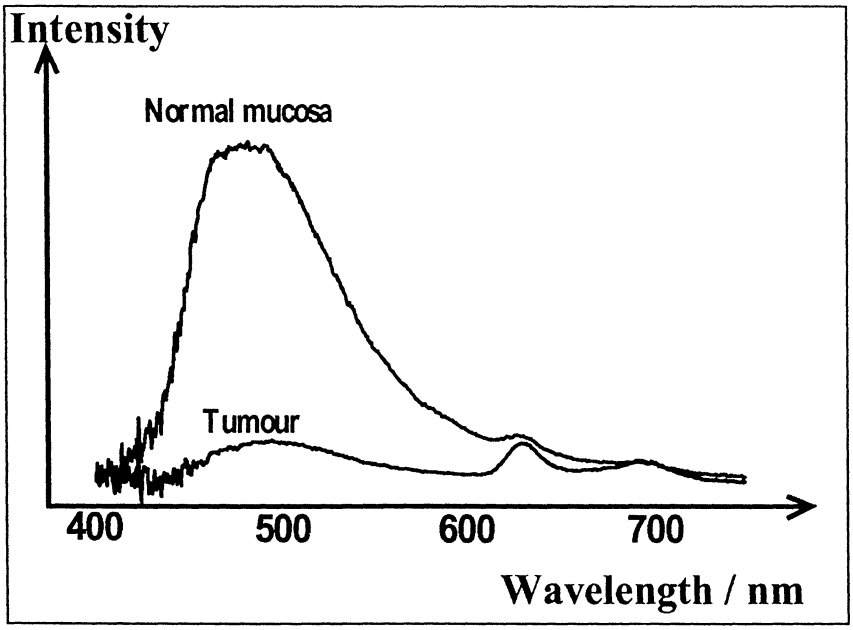

Fig. 2.2. Fluorescence spectra from tumour and normal mucosa.

2.1.3 Treatment

Once demarcated, the tumour is to be treated. One treatment modality based on photochemistry is called photodynamic therapy, PDT. Selected areas are illuminated with light at λ=630-635 nm from for instance a dye-laser pumped by a frequency-doubled Nd:YAG-laser. This light is absorbed by the photosensitiser. The excited molecular complexes of the photosensitisers transfer its excess energy to adjacent oxygen-atoms (due to long lifetime of the excited state). The oxygen-atoms are excited to the singlet state and free radicals are formed. In this state the excited oxygen-atoms are very reactive and oxidate surrounding cells, *e.g.* tumour tissue. Tumour-cell necrosis follows, while it is possible to only mildly and reversibly damaged the

surrounding, healthy tissue. This way of treating cancer, through the use of a photosensitiser and laser light, differs a lot from conventional therapy modality and the only side effect is increased skin sensitivity to light.

2.2 Two-photon excited fluorescence microscopy

It is fairly well known how cell necrosis occurs, but why do the photosensitisers selectively accumulate in tumour tissue? and which cell structures do the photosensitisers bind to and how is it influenced by its surroundings?
Since the photosensitisers are not possible to detect with the naked eye through use of a normal microscope, fluorescence microscopy technique must be used. Two-photon excited fluorescence microscopy is a method under development. This technique might prove to be useful in detecting photosensitisers on a cellular, and hopefully even on a sub-cellular level. This kind of tool is essential for gaining information about the mechanisms behind tumour selectivity, about where in the cell the photosensitises are concentrated and about the behaviour of the photosensitisers inside the cell. It is believed that the photosensitisers are assembled in the mitochondria of preferably malignant cells as well as of epithelial cells in the blood vessels. Several mechanisms are believed to be of importance for the tumour selectivity, *e.g.* shifted ion balance and an increased number of low density lipoprotein receptors in the tumour cells, as well as increased blood vascularisation. For the purpose of investigating this in detail spectroscopic studies of the fluorescence of the photosensitiser is a powerful tool. Performed in combination with two-photon excited fluorescence microscopy technique, high spatial resolution, which is needed for such an investigation, is achieved. [1-6].

2.3 The basis for this paper

When the two-photon project at the Division of Atomic Physics in Lund had come to the point when spectra from different samples could be collected and monitored on a computer-screen, unexpected peaks were observed at various wavelengths (especially at 615-625 nm and 625-640 nm, but also as seen while studied more thoroughly, at 540-560 nm). *Fig. 2.3.* The cause of these peaks was not known, but a non-linear process in the microscope objective was suspected. Amorph materials such as glass are known to be able to yield frequency doubling. [7,8]. Besides the glass, different kinds of glue and anti-reflecting coatings are used inside the objectives. These substances might be the cause of non-linear processes yielding light at these wavelengths. Since two-photon excitation for fluorescence microscopy is a fairly new technique, phenomena of this kind are not yet fully investigated. [9]. The examination of the origin of these unwanted peaks became, together with some related questions, the basis for this diploma paper.

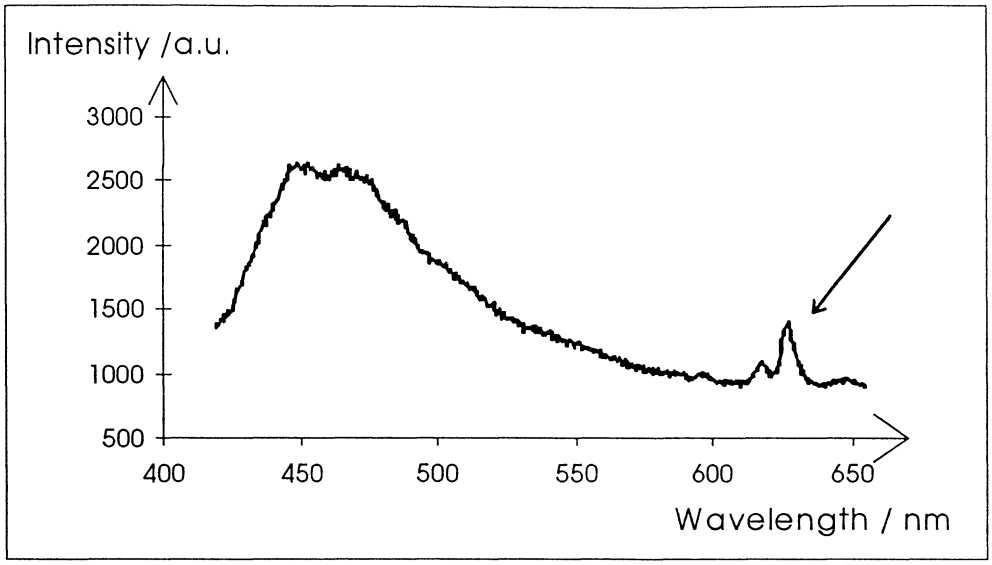

Fig. 1.3. Fluorescence from paper with disturbing peaks. (Pointed out by the arrow).

2.4 Problem description

Microscope objective lenses play a key role in all kinds of microscopy and even more so in the two-photon excited fluorescence microscopy. Not only the monitoring properties such as aberrations, numerical aperture and light-transmission are of interest, but also properties like: "are the lenses emitting background light when used for two-photon excitation, and do such emission vary between different objectives?" or "how much is the laser-pulse broadened when passing through the lens?" Optimising the optics for two-photon excited microscopy, measure the pulse-broadening in the objective and, if necessary, compensate for this broadening with a set of prisms has been one part of this project.

The idea behind the two-photon project is to be able to investigate the localisation and behaviour of photosensitisers in human tissue. A condition for this is the possibility to spectrally resolve the fluorescence and to use that information to demarcate areas containing photosensitisers from those without. Protoporphyrin fluoresces at 635 and 700 nm, where the peak at 635 nm is the stronger one, *Fig. 2.2.* A method to detect ALA is preferably based on this characteristic peak. One of the disturbing peaks in the system was located at 620-640 nm. To be able to measure pure fluorescence spectra from a specimen, one has to get rid of these disturbing peaks. Especially those peaks interfering with the photosensitiser-peaks have to be avoided, in order to increase the sensitivity in the detection of the characteristic protoporphyrin peaks.

Another question discussed in this paper is the size of the focal-point when the beam is focused by a microscope objective. This is interesting because the smaller the size the higher the peak intensity, yielding more efficient two-photon excitation. Likewise in the focal-plane only the fluorophore/photosensitiser in focus is bleached. As mentioned in chapter 3.5 the focal-point in a two-photon process is believed to be smaller than in a single-photon process. The question concerning the size of the focal-point in the two-photon case has been discussed frequently on a theoretical basis in various papers. In this paper experimental results concerning the size of the focal-point in a two-photon process is presented.

3. Theory

3.1 Two-photon excitation

In two-photon excited fluorescence microscopy, two incident photons are simultaneously absorbed to excite a molecule from the ground state to an excited state. This is done without using any real intermediate states. The excited molecule jumps back to the ground state by emitting one photon. The range of energies of the fluorescence photons covers the region up to approximately twice the energy of the exciting light. According to the selection-rules of angular momentum of the molecule, different molecular states are populated in the molecule using two-photon and single-photon techniques [1]. Whether this has any practical interest is not clear because these molecules are complex with a multitude of rotational and vibrational levels degenerating into what resembles a continuum of energy-levels.
Two-photon excitation of an electronic state is achieved via the third-order susceptibility. The transition strength is thus very weak and displays a power-squared dependence upon the intensity. [10]
The original idea of two-photon absorption processes was presented by M. Goepert-Mayers as early as in 1931. [1] The idea of two-photon excited fluorescence microscopy was proposed by Sheppard *et al.* in 1977 [11,12]. In 1990 a method was developed for non-linear excitation in laser scanning microscopy. [13-17]

3.2 Two-photon excitation vs. single-photon excitation.

3.2.1 Image formation

The intensity in the focal region of an aberration-free lens of circular aperture is described by [18]:

$$I(u,v) = \left| 2\int_0^1 J_0(v,\rho)\exp(\frac{1}{2}iu\rho^2)\rho d\rho \right|^2 \qquad (3.1)$$

where the axial and radial normalised optical co-ordinates are given by

$$\begin{aligned} u &= 4kz\sin^2(\alpha/2) \\ v &= kr\sin\alpha \end{aligned} \qquad (3.2)$$

with $k = 2\pi/\lambda$ and $\sin\alpha$ as the so called numerical aperture of the lens.
In a two-photon process with incident wavelength 2λ and assumed fluorescence wavelength λ, the image of a point object is given by Point Spread Function (PSF). The

point spread function describes how an imaging system spreads or distorts the image of a point object. (The concepts numerical aperture and PSF are further explained in appendix A.) The fluorescence intensity as a function of position for a two-photon excitation process is given by [19]

$$I_{(2p)}(u,v) = I^2(u/2, v/2) \tag{3.3}$$

If we only consider the focal plane the expressions for the intensity reduce to

$$I(v) = \left[\frac{2J_1(v)}{v}\right]^2 \tag{3.4}$$

$$I_{(2p)}(v) = \left[\frac{2J_1(v/2)}{v/2}\right]^4 \tag{3.5}$$

The width of the two-photon process response is larger than that of the single-photon process at half the wavelength, as can be seen in *Fig. 3.2,* but in return the intensity of the outer rings is reduced.
The transfer function or Optical Transfer Function (OTF, explained in appendix A) of a conventional fluorescent microscope is [20]:

$$\Lambda(v) = \frac{2}{\pi}\left(\arccos\left(\frac{\lambda F v}{D}\right) - \frac{\lambda F v}{D}\sqrt{1-\left(\frac{\lambda F v}{D}\right)^2}\right) \tag{3.6}$$

This is the expression for a convolution between two circles, where F is the focal length of the lens, D is the lens diameter and v is the spatial frequency.

For a two-photon process the OTF is given by a convolution of two such functions [19]:

$$\Lambda_{(2p)}(v) = \Lambda(2v) * \Lambda(2v) \tag{3.7}$$

where $*$ denote a two dimensional, radially symmetric, convolution. The OTF's of single- and two-photon imaging modes are shown in *Fig. 3.2.* As can be seen, the spatial frequency response is slightly poorer in the two-photon case even though the spatial frequency cut-offs are equal for single-, and two-photon processes and double the excitation wavelength is used.

3.2.2 Confocal two-photon excitation

If a pinhole is introduced into the system in front of the detector, we have a confocal microscope. The idea of a confocal microscope is that rather than, as in a conventional microscope, excitation light from an extended region in the focal plane reaching the detector, all light except from a confined region is retained by an aperture. Confocal microscopy allows direct, non-intrusive visualisation of three-dimensional structures in material. The technique is illustrated in *Fig. 3.1.* The size of the illuminated spot is determined by diffraction in the optics and is typically in the order of $0.5\,\mu m$. The fluorescent light from the specimen is focused onto a small aperture, typically of a diameter of 10-50 μm [20].

In comparison, the set-up used in this project had a slit situated in front of the spectrometer with a width of 25-125 μm. The imaging properties of the current set-up should end up somewhere between the properties of conventional and confocal two-photon exciting technique. Therefore it is of theoretical interest to compare conventional two-photon imaging properties with those of the confocal two-photon case.[21]

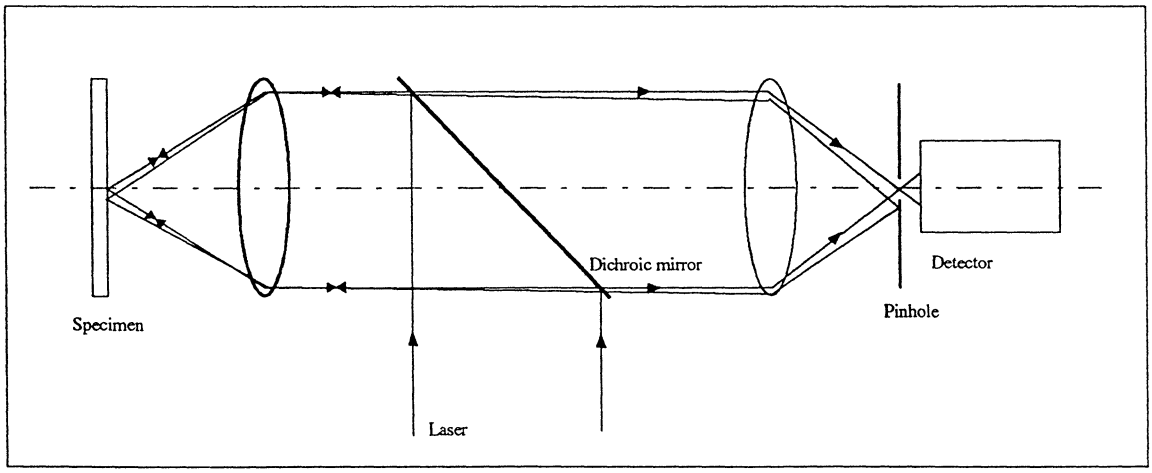

Fig 3.1 Principle of a confocal microscope [20].

In the confocal and the confocal two-photon case the equations for the point spread function look like [19]

$$I_{(cf)}(u,v) = I^2(u,v) \tag{3.8}$$

$$I_{(c2p)}(u,v) = I^2(u/2, v/2) \cdot I(u,v) \tag{3.9}$$

In the focal plane we get the following point spread functions:

$$I_{(cf)}(v) = \left[\frac{2J_1(v)}{v}\right]^4 \tag{3.10}$$

$$I_{(c2p)}(v) = \left[\frac{2J_1(v/2)}{v/2}\right]^4 \cdot \left[\frac{2J_1(v)}{v}\right]^2 \tag{3.11}$$

The point spread functions for the different techniques can be seen in *Fig. 3.2.*

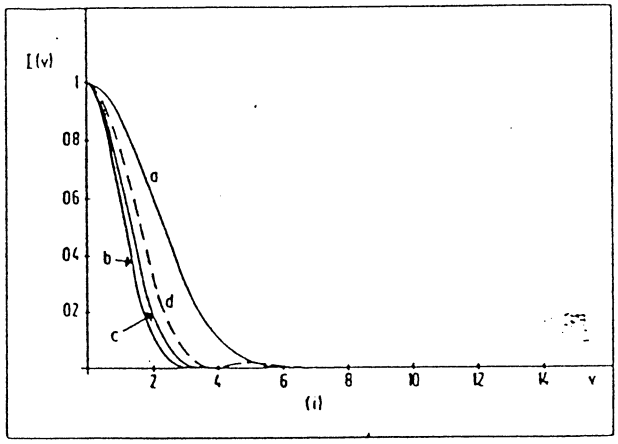

Fig. 3.2. The image of a point object (PSF) in various imaging modes [19]:
(a) two-photon fluorescence
(b) confocal fluorescence
(c) confocal two-photon fluorescence
(d) conventional fluorescence

The corresponding transfer functions for the confocal and the confocal two-photon case consequently are [19]:

$$\Lambda_{(cf)}(v) = \Lambda(v) * \Lambda(v) \tag{3.12}$$

$$\Lambda_{(c2p)}(v) = \Lambda(2v) * \Lambda(2v) * \Lambda(v) \tag{3.13}$$

The spatial frequency cut-offs for the confocal single-photon case and the confocal two-photon case are equal, *Fig. 3.3.* As for the conventional technique, the spatial frequency response is poorer in the two-photon case.

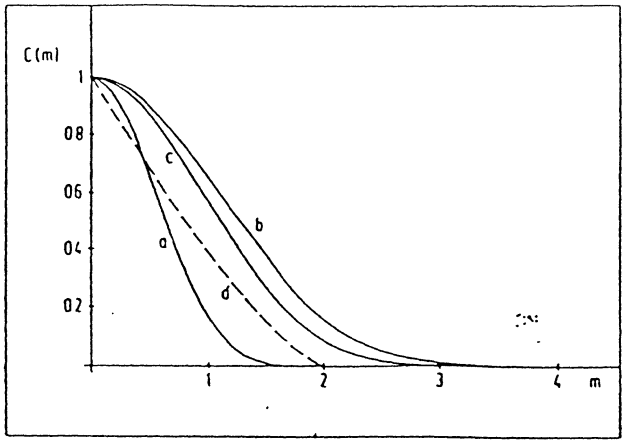

Fig. 3.3. The OTF for various imaging modes [19]:
(a) two-photon fluorescence
(b) confocal fluorescence
(c) confocal two-photon fluorescence
(d) conventional fluorescence

3.3 Depth resolution

Conventional fluorescence microscopy has constant image intensity along the z-axis (no concern taken to absorption and z-axis parallel with the optical axis) which means that no optical sectioning is obtained. (There is no possibility to resolve any spatial frequencies in the z-direction, as is seen in *Fig. 3.4a.* This is referred to as the missing cone [22]). The 3D OTF for single and two-photon systems with excitation wavelengths λ and 2λ respectively, can be calculated as [23]:

$$\text{single-photon: } |\nu_z| = \left(1 - \frac{\nu_r}{2}\right) \cdot \nu_r \tag{3.14}$$

$$\text{two-photon: } |\nu_z| = \begin{cases} 1 & ;0 \le \nu_r \le 1 \\ \nu_r - \dfrac{\nu_r}{2} & ;1 < \nu_r < 2 \end{cases} \tag{3.15}$$

with ν_r and ν_z denoting the lateral and longitudinal spatial frequencies. The 3D OTF is shown in *Figs. 3.4a* and *3.4b*. The missing cone is clearly seen in the single-photon case, as well as that the cut-off frequency is equal in the two excitation methods.

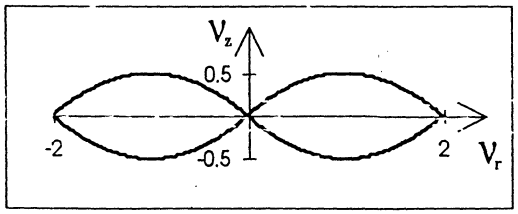

Fig. 3.4a. 3D spatial-frequency bands of a single-photon excitation system. [23]

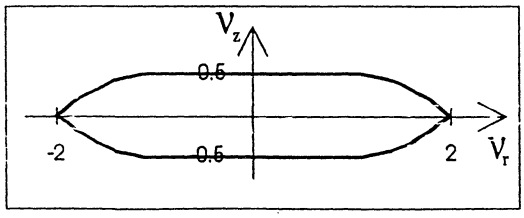

Fig. 3.4b. 3D spatial-frequency band of a two-photon excitation system. [23]

Longitudinal spatial frequency components can only be visualised using conventional or confocal two-photon techniques or confocal single-photon technique. The two-photon technique has intrinsic depth resolution while confocal technique relies on the spatial filtration of the detected signal. These three optical sectioning techniques can be evaluated through integrating the intensity in the image of a single spot in the focal plane, through this operation the axial resolution can be investigated [19]:

$$I_{(cf)}(u) = \int_0^\infty I^2(u,v)vdv \tag{3.16}$$

$$I_{(2p)}(u) = \int_0^\infty I^2(u/2,v/2)vdv \tag{3.17}$$

$$I_{(c2p)}(u) = \int_0^\infty I^2(u/2,v/2)\,I(u,v)vdv \tag{3.18}$$

In *Fig. 3.5* these functions are plotted, it is shown that the conventional two-photon fluorescence method has lower axial resolution than both the confocal methods.
Theoretically the confocal two-photon technique gives a more confined PSF than conventional two-photon technique resulting in higher resolution in both lateral and longitudinal directions. Although an acceptable background rejection is obtained in conventional two-photon technique, it also provides depth discrimination matching confocal microscopy without requiring confocal spatial filter, and thus simplifying the apparatus. [16]

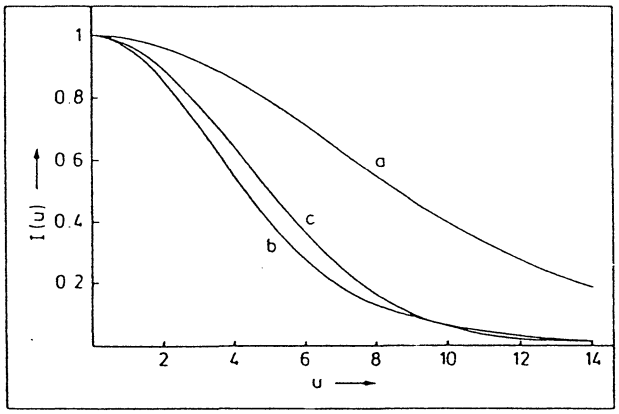

Fig. 3.5. The axial response for a fluorescent plane for [19]:
(a) two-photon fluorescence
(b) confocal fluorescence
(c) confocal two-photon fluorescence

3.4 Focusing

A light-source with a high peak power as well as tight focusing is required in order to obtain a detectable two-photon signal. The excitation light intensity (for single-photon absorption) and the intensity squared (for two-photon absorption) are shown in *Fig. 3.6.* The calculation is made for a homogenous medium assuming we have a diffraction-limited plane-wave. This illustrates the relative fluorescence that excitation yields in the two cases. The plane shown in the figure includes the optical axis.

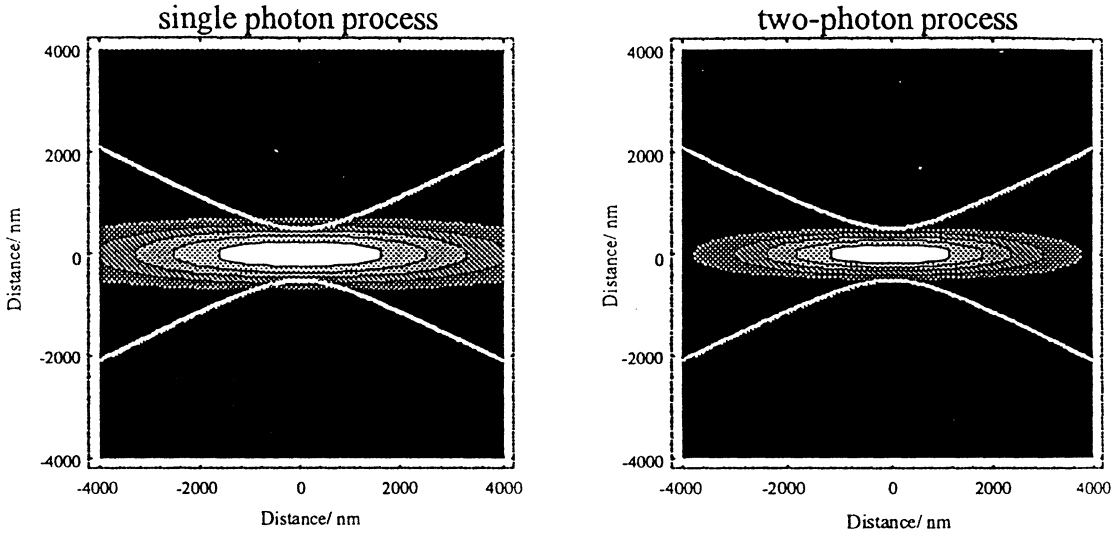

Fig. 3.6. Schematic illustration of the fluorescent volume for one- and two-photon excitation, using a diffraction-limited, focused laser beam. [24]

The light intensity, neglecting the absorption in the medium is given, in cylindrical co-ordinates, by

$$I(\rho,z)=\frac{2P}{\pi\omega^2(z)}\exp\left(-\frac{2\rho^2}{\omega^2(z)}\right) \tag{3.19}$$

with the beam-radius $\omega(z)$

$$\omega(z)=\frac{\lambda}{\pi\cdot N.A.}\sqrt{1+\left(\frac{4\pi\cdot N.A.^2 z}{\lambda}\right)^2} \tag{3.20}$$

where N.A. denotes the numerical aperture for the focusing lens. The calculations were made for a lens with N.A. = 0.45 and a wavelength of $\lambda = 794\text{nm}$. In the figure the outer white lines represent the regions where the intensity has dropped to $\frac{1}{e^2}$ of its value on

the optical axis. The grey-scale represents the fluorescence signal values in a linear scale calculated as $S(\rho,z) = I(\rho,z)$ and $S(\rho,z) = I^2(\rho,z)$ for one- and two-photon excitation, respectively. The outermost ellipsoids give the borders at which the signal is $S(\rho,z) = \frac{1}{e^2}S(0,0)$. For the two-photon signal the cross-section of the volume has a diameter of 0.9 μm and the length of 7.2 μm. [24].

3.5 Photobleaching

Photobleaching is a problem in all fluorescence imaging. Whether the specimen is stained with a fluorophore, like in conventional fluorescence microscopy, or if it contains photosensitisers, the fluorescence always fade while the sample is illuminated. (*Fig. 3.6*). Photobleaching is usually a considerable nuisance, particularly in quantitative studies, and therefore minimising it is of great importance. [25] The excited volume is smaller in two-photon excited fluorescence microscopy than in both conventional and confocal single-photon microscopy, because the bleaching depends on the square of the intensity. The bleaching along the optical axis falls off strongly above and below the focal plane, (as $1/z^2$ for large z). [13] Still, the mechanisms behind photobleaching are very complex and the process is dependent on various factors connected to the type of fluorophore used and its physical-chemical micro environment.[26]
Another advantage of the two-photon excited method is that using 792 nm instead of 396 nm as exciting wavelength might yield deeper penetration in tissue. This is due to the light-absorption in haemoglobin which is approximately 1000 times higher for 396 nm than for 792 nm [1]. The uncertainty is due to that the two-photon excitation is critically dependent of the excitation peak power, reduced with depth by light scattering.

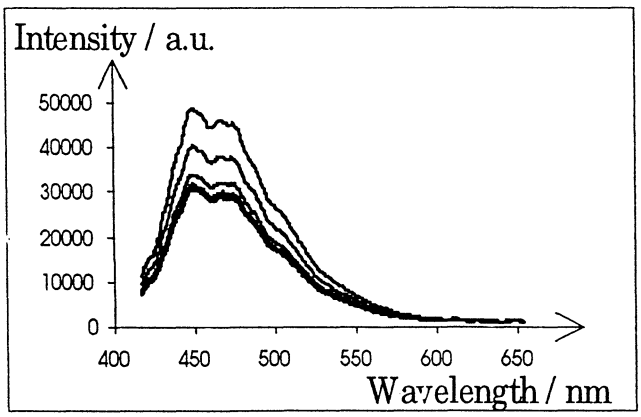

*Fig. 3.6. Bleaching of the fluorescence from a paper sample; the signal level clearly decreases between the measurements. The detection time was 5*10 sec.*

3.6 Chromatic aberration

Microscope objective lenses are compensated for chromatic aberration in one specific wavelength region, therefore special optics are required for excitation in the UV-region. (Appendix B) Designing objectives for the UV-region is more complicated than for the visible region and the result is often poorer. Special optics are not supposed to be necessary when using two-photon technique since the wavelength of the incident photons is 792 nm and the fluorescence light between 400 and 700 nm.

3.7 Theoretical considerations - summary

Confocal single-photon, conventional or confocal two-photon excitation technique have to be used in order to obtain depth resolution. Due to the squared intensity dependence of the two-photon excitation techniques, the fluorescing volume in the focal region and hence the spatial resolution is better in the two-photon case. Furthermore, photobleaching is less extended while using two-photon excitation technique.
The confocal technique has a more confined point spread function, yielding higher resolution and higher spatial resolution, than conventional techniques. A pure confocal two-photon excited fluorescence microscopy set-up is however more difficult to adjust due to the pinhole and thus less robust than the set-up used in this project.

4. Materials and methods

4.1 Introduction

The two-photon excited signal is much weaker than the single-photon signal, it is impossible to detect such signals in normal fluorescence microscopy. Furthermore, if exciting with a wavelength 2λ, (*Fig. 4.1*), conventional single-photon excited fluorescence is detected using a filter to cut off the laser-light. The filter cuts all light with shorter wavelengths than $2\lambda + \Delta\lambda$ which means that a possible two-photon signal is impossible to detect in normal fluorescence microscopy. In our set-up the different kind of filter that is used makes it possible to detect wavelengths shorter than the one of the incident light. A band-pass filter that transmits light with wavelengths between λ and $2\lambda - \Delta\lambda$, keeps the laser-light out and still makes it possible to detect the two-photon signal is used.

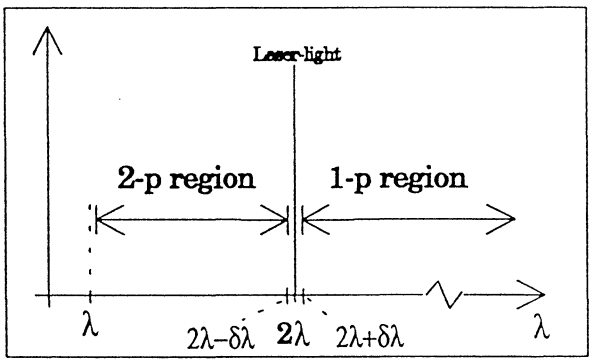

Fig 4.1. Schematic of single- and two-photon excited detection regions.

4.2 Microscopic arrangement, spectroscopic mode

The arrangement for the two-photon excited fluorescence microscopy with spectrally resolved detection is shown in *Fig 4.2*. The 792 nm light from the Ti:sapphire laser is led through the fluorescence excitation light port of the microscope to a dichroic mirror reflecting the laser light while transmitting the signal. This mirror reflects the incoming light onto the sample, which then fluoresce at wavelengths 400 nm and longer. (Light at shorter wavelength than 400 nm is reflected/absorbed by the dichroic mirror. This light, however, is of no interest since no fluorescence below 396 nm is emitted due to the Stoke-shift towards longer wavelengths compared with the exciting light). The fluorescence-light, collected with the microscope lens used to focus the exciting light, will be focused onto the entrance-slit of the spectrometer. Before entering the spectrometer, the light is filtered through a 2 mm BG39 Schott-filter (transmission between 320 and 700 nm) to eliminate any scattered light from the laser. The spectrally resolved signal is then detected by a CCD camera at the exit plane of a spectrometer.

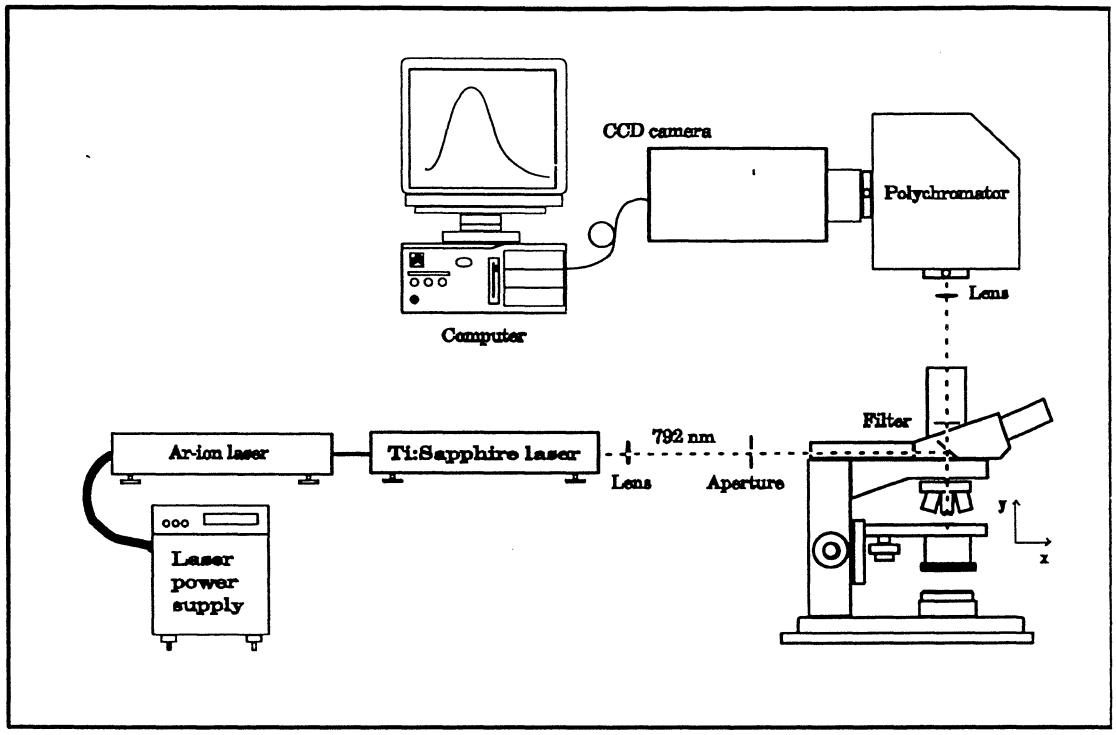

Fig. 4.2. Arrangement for two-photon excited fluorescence microscopy, spectroscopic mode.

4.2.1 The light source

To generate a two-photon process that gives a signal strong enough to detect, a very high peak-power is required. On the other hand, the average power reaching the sample has to be low to avoid heating the sample. To fulfil these two requirements a pulsed laser must be used and in this set-up a Ti:sapphire (Coherent MIRA 900) mode-locked by a Kerr-lens and pumped by a continuos Ar:ion laser (Coherent Innova 400) is utilised. With a pulse-width of 150 fs, a repetition rate of 76 MHz and an average effect of about 40 mW (of which 13 mW remains after the pulse has passed the optical components), a maximum peak-power of more than 1000 W is obtained. This gives a peak-intensity in the focal-point of $2.8 \cdot 10^{11}$ W cm^{-2} for a fully illuminated lens with N.A. = 0.45, if the laser-beam is approximated to a diffraction-limited plane wave. The Fourier-limited band-width is 6 nm. The wavelength of the Ti:sapphire laser can be tuned between 760 and 840 nm. In this project λ = 792 nm was used. [27,28]

4.2.2 The microscope

A conventional Nikon Labophot-2 microscope, schematically shown in *Fig. 4.3* was used to focus the laser-light onto the specimen and collect the fluorescent light. Labophot-2 is an epi-fluorescence microscope which means that the specimen is both illuminated (normally with a Hg-lamp) and observed through the eye-piece, from above. With Labophot-2 it is possible to use an alternative light-source. The exciting light enters from behind and is focused by the microscope lens, onto the specimen. The fluorescence light is then either observed by the naked eye, or guided past the eye-piece onto any detection system.

The microscope is equipped with a scanning stage (Märzhäuser Wetzlar EK32) that can be controlled from a computer or by a joystick. This stage makes it possible to record images of the specimen while scanned like shown in *Fig. 4.3.*

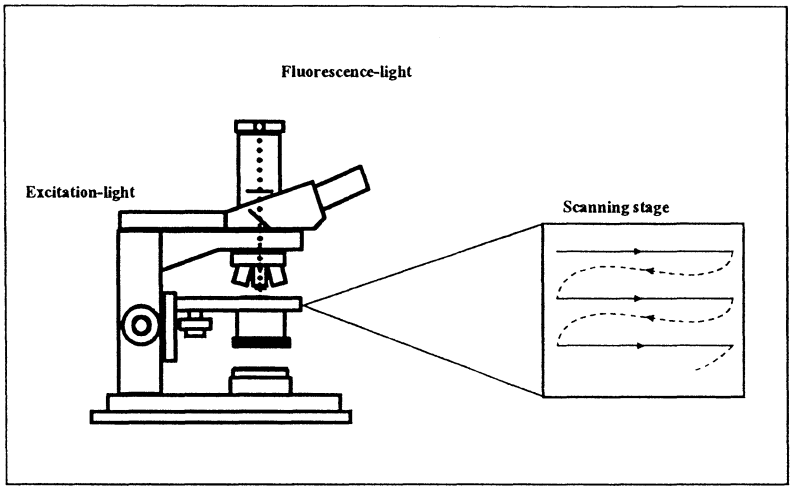

Fig. 4.3. Schematic of microscope and scanning stage.

4.2.3 Microscope objective lenses

A microscope objective lens is specified by its magnification, its numerical aperture, (N.A.), and its immersion medium. There is also a difference in what kinds of aberrations the objective is compensated for. The immersion medium is the medium between the specimen and the microscope objective (normally air, water or oil). There is a multitude of different types of objectives made for different application and varying in price. Depending on aberration corrections, objectives can be classified into the following categories, in order of rising cost and performance:

- Achromats
- Flat-field (or plan) achromats
- Fluorites
- Flat -field (or plan) fluorites
- Apochromats
- Flat-field (or plan) apochromats.

Achromats are colour-corrected for a relatively narrow wavelength range, while fluorites and, especially, apochromats are useful over a wide range. "Flat-field" means that the field-curvature of the objective is very small. [20] A thorough explanation of field curvature and chromatic aberration is given in appendix B.
Finding the optimal microscope objective lens for two-photon microscopy has been of great interest, therefore a variety of different lenses have been used and examined. The following ones are all from Nikon, and the immersion medium is air [29].

- *CF E Achromat 10/0.25*, (magnification 10x and N.A., 0.25). This is the basic achromat objective.

- *CF Plan Achromat NCG 40/0.65*. Designed for use without cover-glass.

- *CF E Plan Achromat 10/0.25 and 40/0.65*.

- *CF N Plan Achromat 40/0.7*.

- *CF N Plan Apochromat 10/0.45 and 20/0.75*. The Plan Apo lenses features extra-high light transmission and provide chromatic aberration correction across the entire visible region.

- *CF Epi-Fluorescence Fluor 20/0.75 and 40/0.85*. Light-transmission extending into the ultra-violet region (down to 340 nm). It is designed especially for low-light fluorescence images.

4.2.4 The spectrometer

A spectrometer (SPEX 270M), shown in *Fig. 4.4*, is used to resolve the fluorescence signal from the sample into its spectral components. This in done by a grating with 150 grooves per mm (first order), blazed at 500 nm, and two mirrors. The focal length is 0.27 m, f/4, and slit widths between 25 and 125 μm were used.

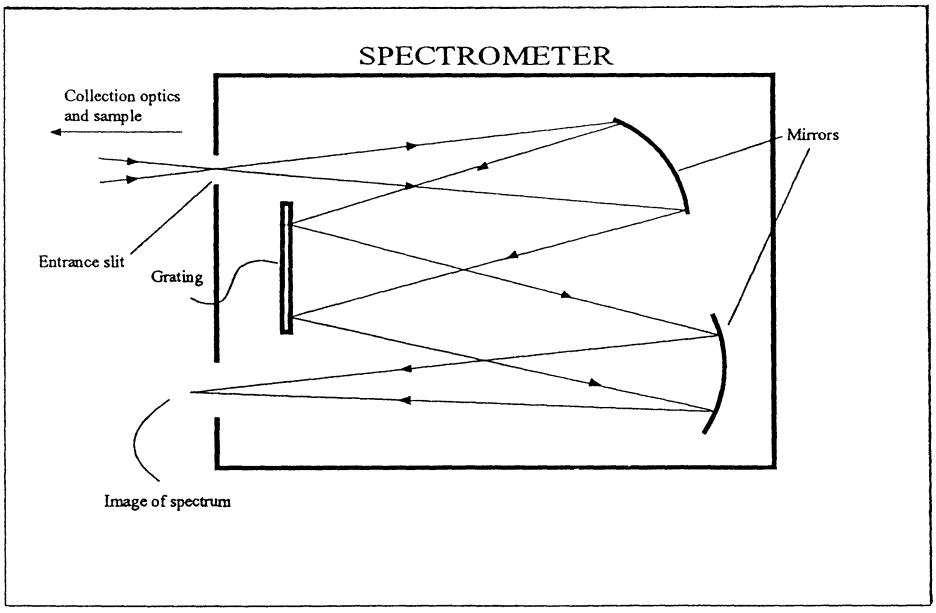

Fig. 4.4. Schematic illustration of a spectrometer.

4.2.5 Detection

Two different techniques were used to detect the signals from the sample. The most frequently used technique in this project was to detect the spectrally resolved image with a CCD-camera (EG&G Parc OMA 4000). (CCD = Charged Coupled Device). The CCD-camera used can be seen as a linear array of 512 photodiodes. Each photodiode collects the incoming light during a chosen integrating time and the signal

is then read out to an Optical Multichannel Analyser system, (OMA-4000) and represented as a graph on a screen. The signal out from each of the 512 elements is proportional to the incoming light. Through this technique it was possible to monitor the total spectral information in semi real-time on a computer screen. To minimise the dark-current the CCD-camera is cooled with liquid nitrogen. Some cross-talk between adjacent elements in the CCD is inevitable and this decreases the resolution. The spectral resolution of the system was about 20 nm. Typical integration times used in the spectra shown was 10 or 100 seconds.

4.3 Microscopic arrangement, imaging mode

While working with the equipment in imaging mode (as schematically shown in *Fig. 4.5.*) the light was guided the same way as in the previously described arrangement. The detection method differ however; the fluorescence light is detected with a photomultiplier tube, PMT, (Hamamatsu R928) while the stage of the microscope was scanned over the previously defined area. The current from the PMT was monitored using an oscilloscope and the information was displayed on a computer screen as a fluorescence image. Regions of interest on the image can then be studied with the previously described spectrally resolved detection method.

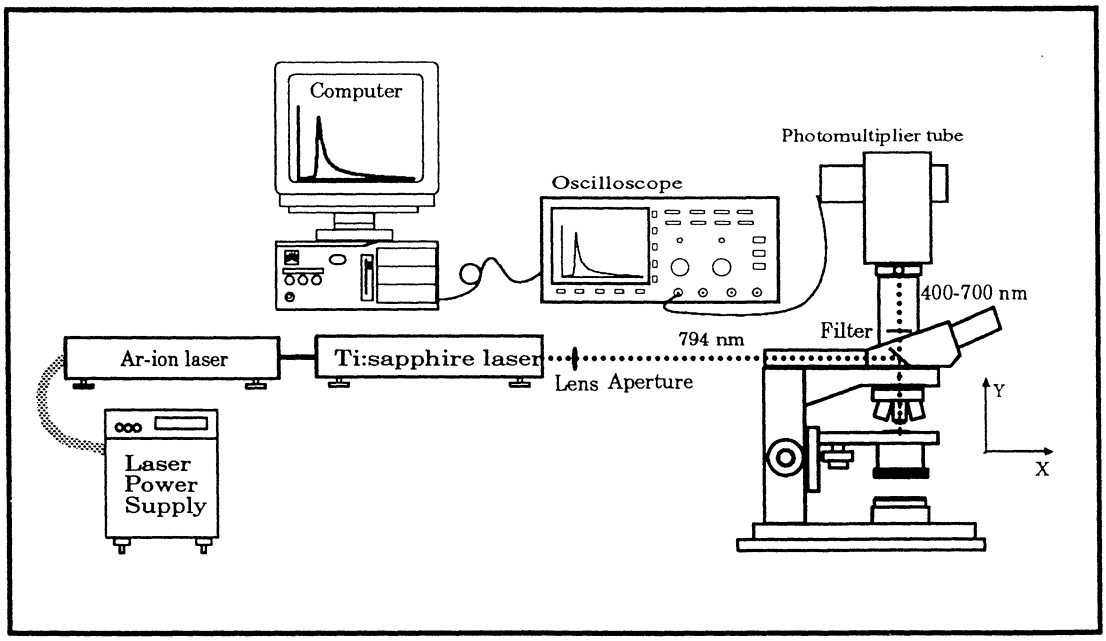

Fig. 4.5. Arrangement for two-photon excited fluorescence microscopy, imaging mode.

4.3.1 The oscilloscope

A Tektronix TDS 520A two channel digitising oscilloscope was used to convert the signals from the photomultiplier tube to information possible to store pixel by pixel, in the computer memory. The oscilloscope sample the signals from one scanned row (*Fig. 4.3*) and divide it into the number of pixels partitioned for each row of the image. (A typical number is 25 measured points form one pixel).

The oscilloscope was also used for detecting the signal from the autocorrelator while measuring the pulse-broadening.

4.4 Autocorrelator arrangement

In order to measure the pulse-broadening in the microscope optics, light from the Ti:sapphire laser was guided through two microscope objectives (Plan Apo 10/0.45 and Plan Apo 20/0.75) and the pulse-width was measured with an autocorrelator connected to an oscilloscope and a computer. As seen in *Fig. 4.6*, the two lenses were arrayed like in a x-y-z positioning frame. The beam-divergence after the microscope lenses was minimised using a He-Ne laser. This was done through positioning the lenses on a straight line with a separation of twice the focal distance, so that the focal-points of the two lenses coincided.

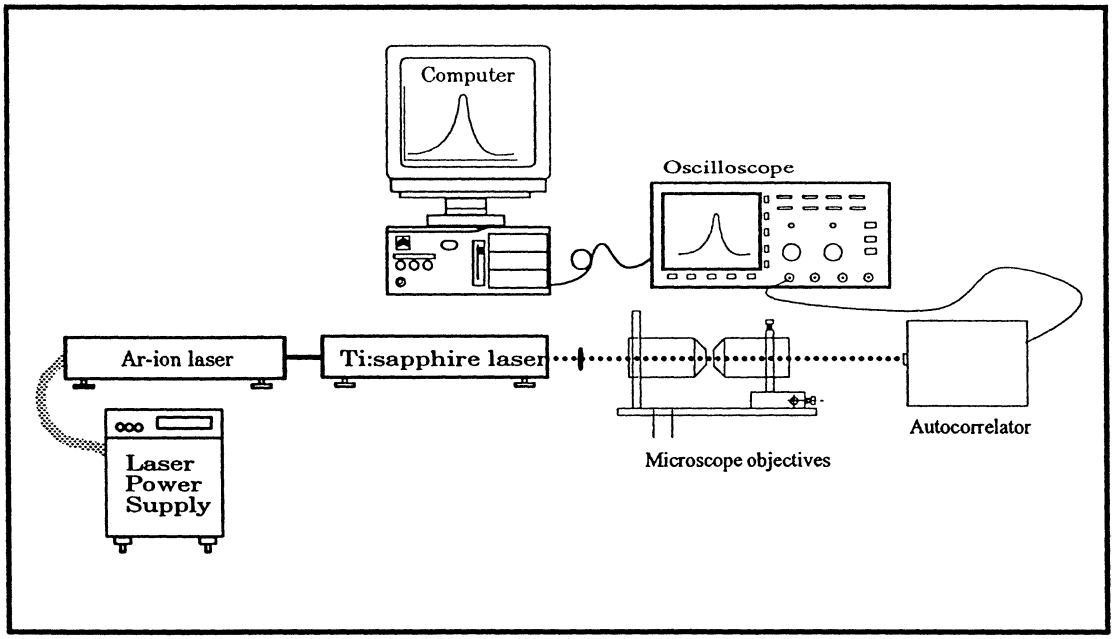

Fig. 4.6.. Set-up for measurement of pulse-broadening in microscope objectives.

4.4.1 The autocorrelator

A scanning autocorrelator (Femtochrome Research Inc. FR-103XL, shown in *Fig. 4.7* [30], was used in the pulse broadening measurements). It is a high resolution instrument for continuous monitoring and displaying of femtosecond and picosecond laser-pulses. The standard operation wavelength is 460-1200 nm. The pulse width resolution is about 50 fs. This autocorrelator uses second-harmonic generation (SHG) of the first kind in the conventional Michelson interferometer set-up for pulse width measurement. Repetitive linear delay generation in one arm of the Michelson arrangement is achieved by a pair of parallel mirrors centred on a rotating shaft. The rotation of the parallel mirror assembly leads to an increase (or decrease) of the pathlength for a traversing beam. The transmitted pulse train is thus delayed (or

advanced) about the reference (zero delay). This delay varies with time as a function of the shafts rotation.

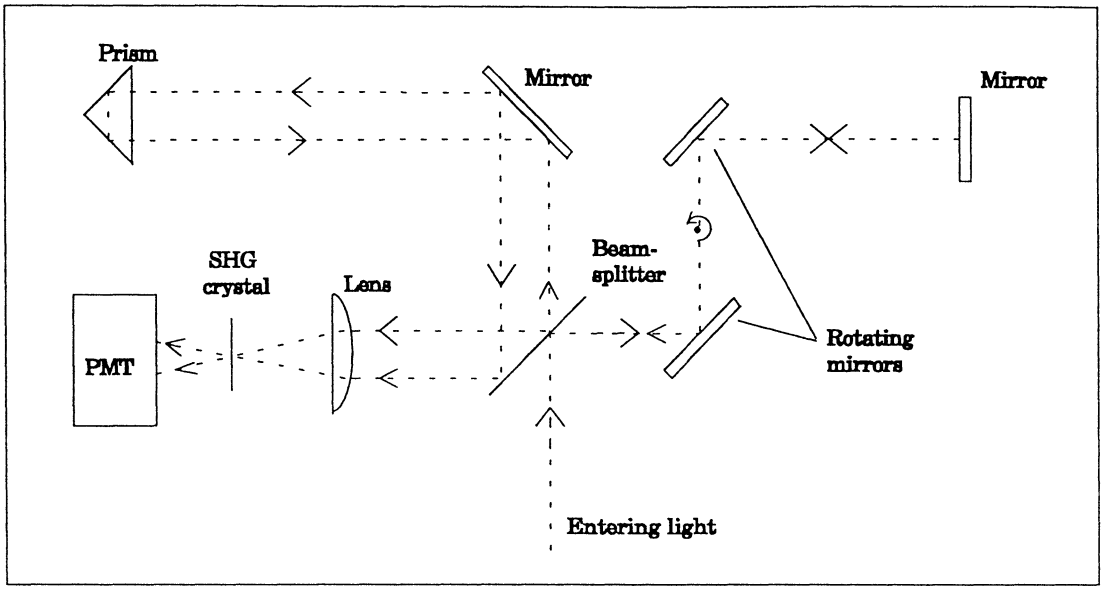

Fig. 4.7. Schematic of the autocorrelator Femtochrome research inc. FR-103XL..

4.5 Focus-size measurements

To conduct measurements of the size of the focal-point, the specimen movements between the different measurements must be possible to determine at a micrometer scale. In this set-up, a scanning stage was used in the x-y plane and the fine-focus ring on the microscope in the z-direction. A well defined spot of the specimen was illuminated, and hence bleached, during 3-4 minutes. Images of the bleached spot was detected partly in imaging mode and partly fluorescence spectra were recorded at well defined distances from the bleached spot in the spectroscopic mode. Five spectra were recorded around each spot (one at the spot, one below, one above, and two in the focal plane). After studying the bleaching between each measurement it was possible to decide whether that specific spot formed part of the originally bleached focal-point, or not. Since the limits of both the original point and the measured point were somewhat vaguely defined, no exact value for the focal-volume was obtained, rather maximum values that the accurate measures are inferior to.

5. Results

5.1 Optics optimisation and elimination of disturbing peaks.

Normal microscope objective lenses - such as those used in this project - are designed for conventional fluorescence microscopy. Since other qualities are important in the conventional case, it is not obvious which ones that are best suited for two-photon excited fluorescence microscopy. In this project, effort has been concentrated primarily on light transmission properties and to avoid any laser-induced background emission from the optics.

5.1.1 The peaks

The peaks shown in *Fig. 2.3* were found in all collected spectra, independent of the type of sample examined. A couple of possible sources were suspected to be the origin of this disturbance:

- A non-linear process in the microscope objective lenses yielding light in these specific wavelength-regions.
- The laser-light might contain other wavelengths than the expected one at 792 nm that in some way was detected by the CCD-camera.
- Any arbitrary light might enter the system either through the microscope objective or directly through the spectrometer.
- The spectrometer has been known to cause problems before and was therefore suspected to redifract light that could reach the detector [31].
- The origin of the disturbance might be the specimen, although every specimen showed resembling peaks. Non-linear processes have been detected in amorph materials. [7,8]

After a series of measurements, using several different lenses, without any major difference in the peaks, and after discussing the problem with the technological adviser for Nikon Europe in Holland, Mr M. Yoshida, the disturbances was presumed not to be caused by the microscope lenses. Instead the interest was concentrated on the surrounding equipment, such as the spectrometer and the laser.
Finally it stood clear that light from the room where the Ti:sapphire laser was located found its way into the microscopy-lab and into the CCD-camera (light from the Ar:ion laser and scattered room illumination). Also scattered light from the computer (mainly from the screen but also from diodes) entered the system directly through the spectrometer. Light from the Ti:sapphire laser-room could be kept out using apertures, made of black carton, on booth ends of the tube guiding the laser beam into the microscopy-lab. The result can be seen in *Fig. 5.2.*

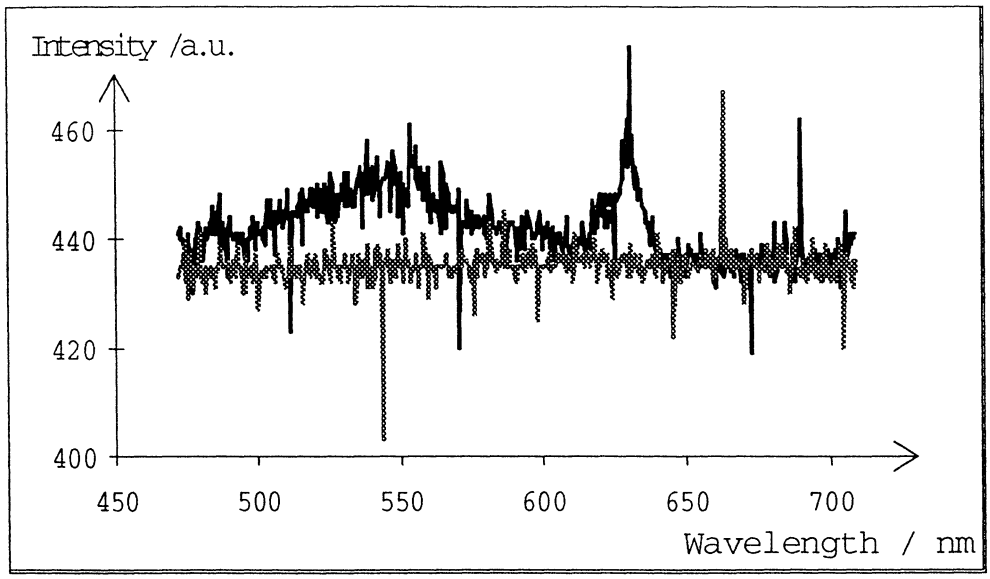

Fig. 5.2. Background signal with external light kept out of the microscopy-lab (grey curve) and the original background signal (black curve).Sample time 10 sec.

Light from the computer entering the system through the spectrometer can be kept out in two ways: either all diodes are covered and the screen is blacked out during the measurements or the path between the exit of the microscope and the entrance of the spectrometer can be enclosed. Using the former method, any light that might enter the lab (for example through a not perfectly tight door-frame) still would enter the system, furthermore it is not a very convenient method. The latter alternative is thus preferred, and it was the intention to incorporate such a permanent construction in this project. However, various uncertainties concerning the future set-up made it impossible to conclude this part of the project. One step towards an enclosed path between the microscope and the spectrometer is however taken. A "periscope" positioned at the exit of the microscope has been designed, *Fig. 5.3.* The next step would be, when the set-up is permanent, to design a "tube" to enclose the remaining path between the periscope and the spectrometer. This was now done using black paper.

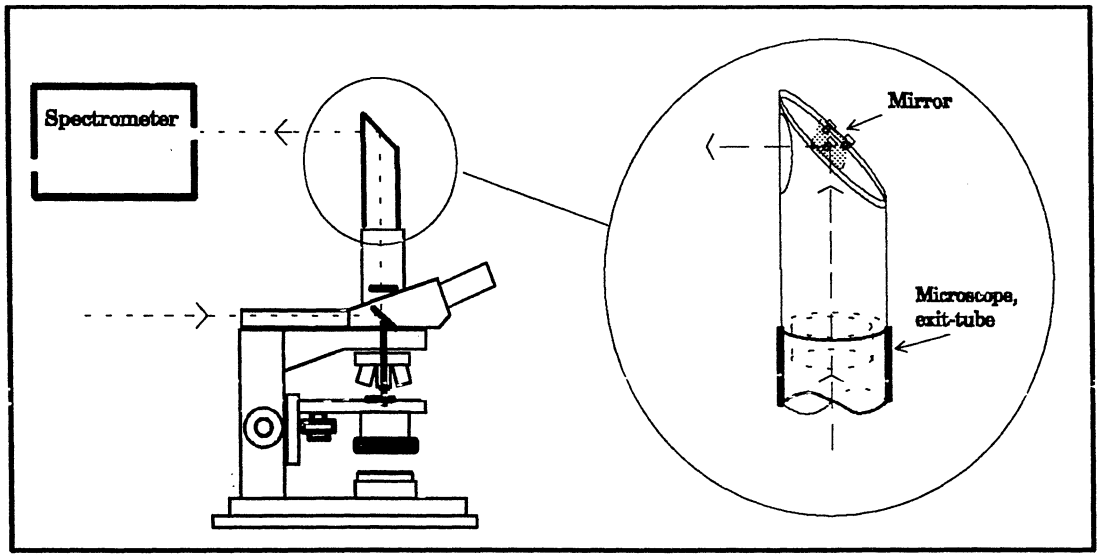

Fig. 5.3. Schematic of the "periscope" designed for the microscopy set-up.

The result from keeping light from the computer out of the system is shown in *Fig. 5.4.* In total, with apertures and the light from the computer kept out, the fluorescence from a paper sample looks like in *Fig. 5.5* (grey curve), in comparison to the spectra obtained before any measures were taken to obliterate the disturbing peaks (black curve).

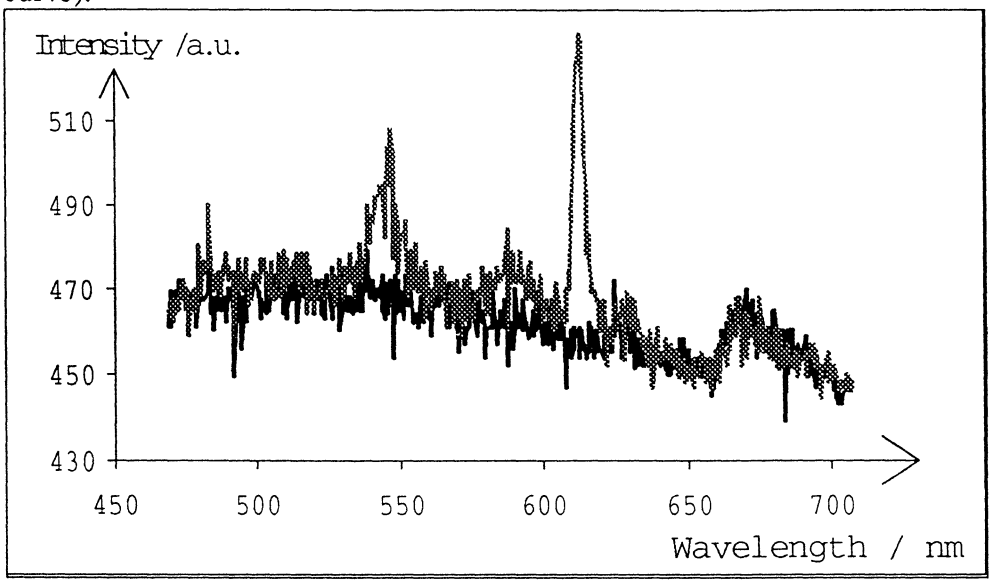

Fig. 5.4. Background signal with and without light from the computer kept out of the system. The integration time was 10 sec.

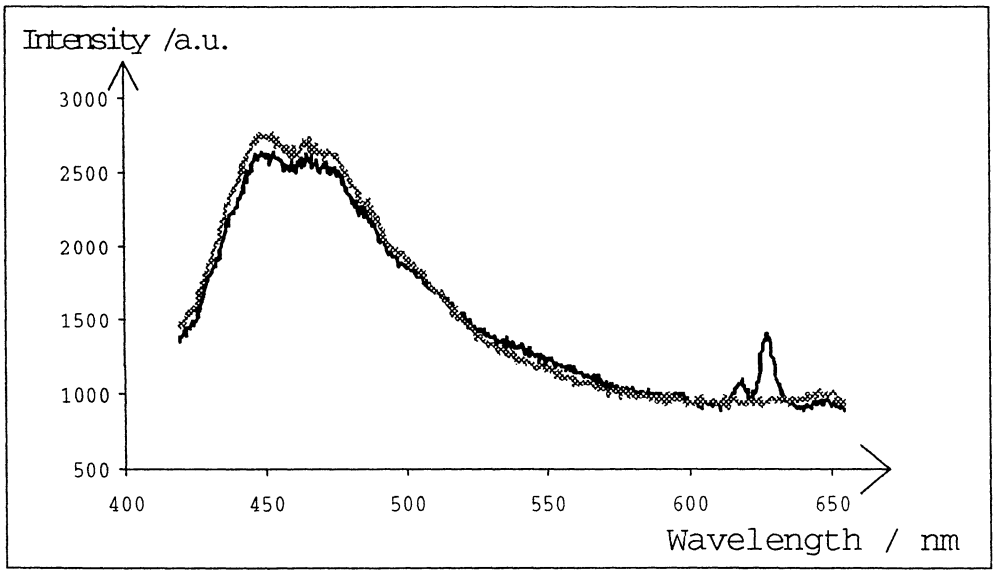

Fig. 5.5. Fluorescence from paper before and after measures were taken to obliterate the disturbing peaks. The integration time was 10 sec..

5.1.2 Optimising microscope objectives

Different objective lens characteristics, of importance for two-photon excited fluorescence microscopy, have been tested for lenses with three magnifications; 10x, 20x and 40x. In the following figures, light-transmission properties of the different objective lenses are plotted. The fluorescence spectra are from paper and liver and the light integration time was 10 or 100 seconds.

Magnification 10x: Three different objective lenses were tested: N Plan Apochromat 10/0.25, (Plan Apo 10x), E Plan Achromat 10/0.25, (E Plan 10x), and E Achromat 10/0.25, (E Achromat 10x). From *Fig. 5.6* it is seen that the N Plan Apochromat objective is to be preferred in terms of transmission.

Magnification 20x: Epi-fluorescence Fluor 20/0.75 (Fluor 20x) and N Plan Apochromat 20/0.75 (Plan Apo 20x) were tested and the Fluor objective showed a slightly better light transmission, see *Fig. 5.7.*

Magnification 40x: Among the four objectives tested in this category, E Plan Achromat 40/0.65, (E Plan 40x), N Plan Achromat 40/0.7, (N Plan 40x), Plan Achromat NCG 40/0.65, (Plan NCG 40x) and Epi-fluorescence Flour 40/0.85, (Fluor 40x) two showed considerably better characteristics: the N Plan Achromat and the Flour objectives. And as is the case with the 20x-objectives, the Flour objective is the better one. *Fig. 5.8a* and *5.8b.*

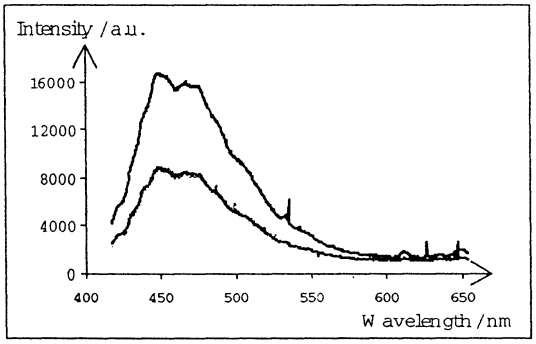

Fig. 5.6. Two-photon signal from paper using Plan Apo 10x (upper black curve), E Plan 10x (lower black curve) and E Achromat 10x(grey curve). (The integration time was 10 sec).

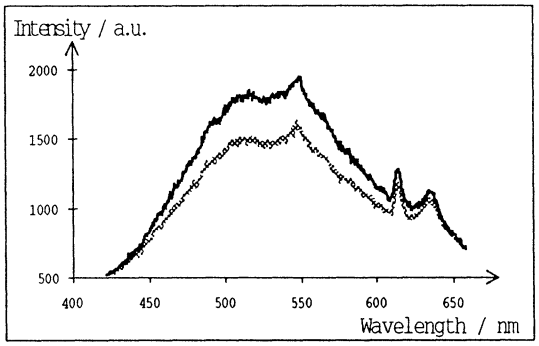

Fig. 5.7. Two-photon signal from liver containing photosensitiser using Fluor 20x (black curve) and Plan Apo 20x (grey curve). (The integration time was 10 sec).

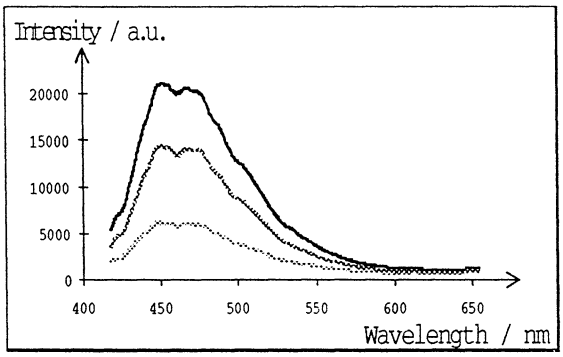

Fig. 5.8a. Two-photon signal from paper using N Plan 40x (black curve), E Plan 40x (grey curve) and Plan NCG 40x (light grey curve). (The integration time was 10 sec)

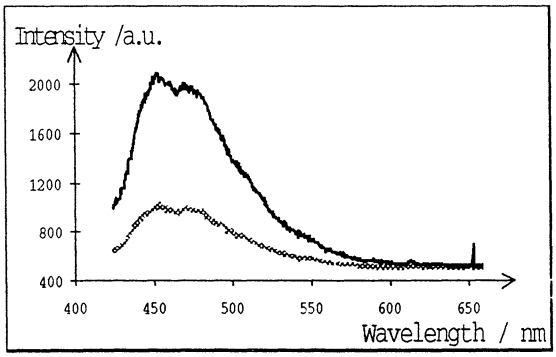

Fig. 5.8b. Two-photon signal from paper using Fluor 40x (black curve) and N Plan 40x (grey curve. (The integration time was 10 sec)

The Flour objectives have the highest light transmission, slightly better than the N Plan Apochromat and the Plan Achromat objectives. But they lack one important property, namely the plane-curvature correction (Appendix B). This is however not very

important when using a scanning stage, as is done in this set-up, but becomes crucial in a scanning beam set-up (Appendix A). Since it is probable that the two-photon fluorescence microscopy set-up will be upgraded with a scanning beam system, objectives with plane-curvature correction are preferable. Moreover, the difference between the Flour and the N Plan Apo objectives is comparatively small. The Fluor 40x is however considerably better than the N Plan 40x.
The objective lenses tested with the highest transmission are for the three magnification categories the N Plan Apochromat 10/0.25 and 20/0.75 and the Fluor 40/0.85.

5.1.3 Pulse broadening

The Ti:sapphire laser generates high peak power pulses with a length of approximately 100 femtoseconds, (fs). To get a detectable two-photon excited fluorescence signal it is very important to maintain the high intensity generated by the laser. The more the pulse is broadened, the lower the peak power (or intensity) gets, and the probability for a two-photon process decreases drastically since this probability depends quadratically on the intensity. Therefore it is necessary to measure the length of the pulse after it has passed through the objective and if the pulse is broadened too much, it is necessary to compensate for this broadening with a set of prisms.
The pulse-length was measured using the set-up described in chapter 4.4 and found to be 120 fs after passing through two microscope objectives (N Plan Apochromat 10x and N Plan Apochromat 20x). The FWHM of the curve in *Fig. 5.9,* shows the autocorrelation curve of the pulse (before decorrelation which is done through multiplying with a factor 0.648 [32]). The pulse is broadened by roughly 10 %, (to 110 fs), after passing one microscope lens assuming that the pulse is broadened equally in the two lenses. The other optical components are not broadening the pulse in a significant way [33]. Any arrangement to counteract this slight broadening was not considered to be necessary.

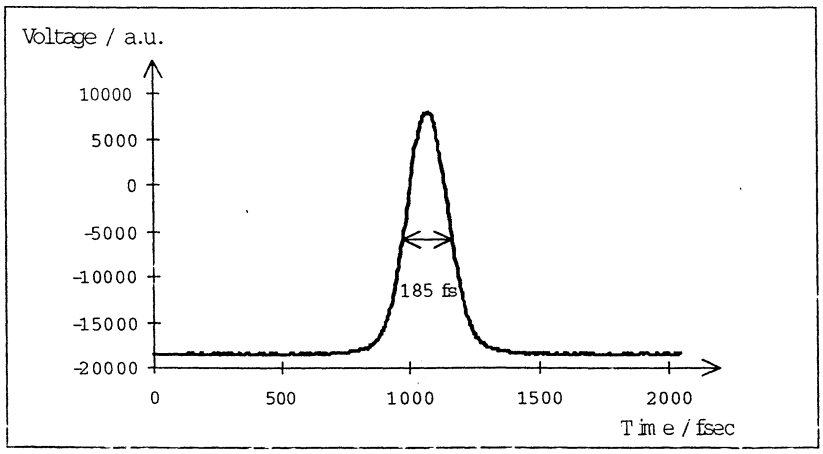

Fig. 5.9. The auto-correlation curve of a laser-pulse that has passed through two microscope lenses.

5.2 Photosensitiser detection

5.2.1 The effect of the laser-pulse

The average effect of the laser-beam used to excite the sample was in this study too high for an immovable sample because it got burnt in focus. There are two different ways to avoid this problem: either the effect of the exciting pulse is decreased by a filter, or the specimen is held in motion while measuring. The former method has been tested using different filters (NG 3, 4 and 5) introduced in the set-up before the microscope. However, the ratio between signal and background (the signal-to-noise, S/N, - ratio) deteriorated too much to make measurements possible and as seen in *Fig. 5.10*, the protoporphyrin-fluorescence signal almost disappeared. The latter method was tried primitively by keeping the specimen in motion using the scanning stage, controlled by a joystick. A better signal was obtained and the sample was prevented from burning, *Fig. 5.12*. A more sophisticated way to do this would be to use the scanning-control program, but using the OMA-system at the same time as the scanning-control program was impossible. A home-made program for the OMA-system would be necessary. The idea of the two-photon project is, however, primarily not to make spectrally resolved fluorescence images, but to make normal fluorescence images without using the OMA-system, (and sometimes to record spectra from certain points). While making such images the specimen is in constant motion and burning do not occur. For spectrally resolved fluorescence spectra the primitive method to avoid burning will have to be used.

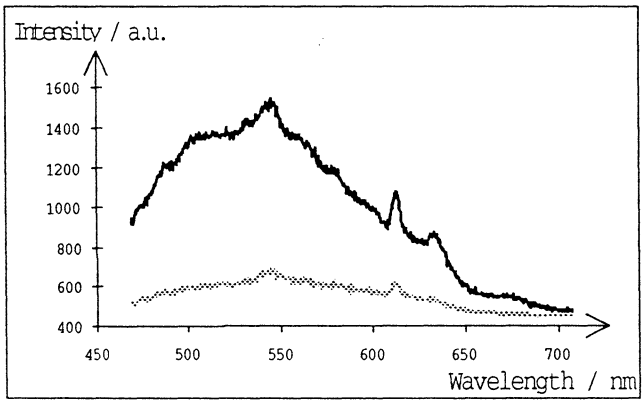

*Fig. 5.10. Fluorescence-signal from ALA-containing liver with **filtered** (grey curve) and **un-filtered** excitation-pulse (black curve). The integration time was 10 seconds.*

5.2.2 Protoporphyrin recognition

Once the disturbing peaks were eliminated, the protoporphyrin detection in tissue was possible. The fluorescence-peak at 635 nm was clearly distinguishable. To obtain a detectable protoporphyrin fluorescence signal, samples of liver from rat injected with ALA as well as normal rat liver tissue were examined. The rat stained with ALA (30 mg/kg body weight) was sacrificed three hours after injection. The removed organs were frozen in isopentane with carbonic ice and then kept at a temperature of -18 °C. No further staining procedures were adopted.

A weak but detectable PpIX-fluorescence signal was obtained from the liver sample from the ALA-injected rat. It was clearly distinguishable from the signal from the untreated sample, *Fig. 5.11*. Due to burning of the sample (described above), and photobleaching (chapter 3.5) a stronger PpIX-peak could be expected if the specimen was kept in motion during measurements. That this is the case can be seen in *Fig. 5.12* where the fluorescence signal from rat-liver when the samples were kept in motion during the measurements is shown.

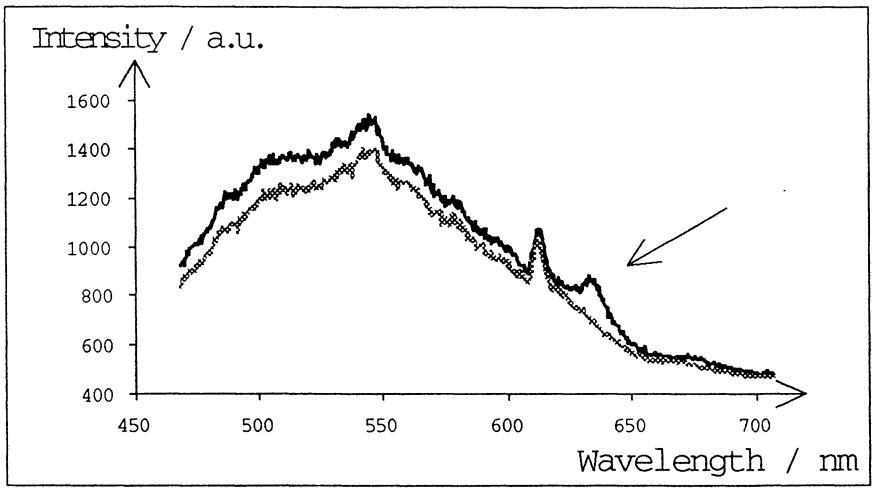

Fig. 5.11. Fluorescence-signal from normal (grey curve) and ALA-injected liver-sample (black curve). The arrow points out the PpIX-peak. The integration time was 10 sec.

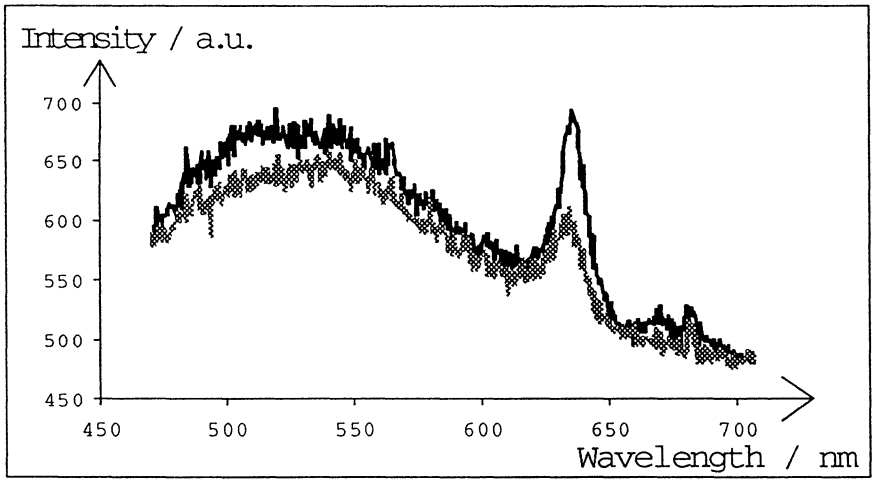

Fig. 5.12. Fluorescence-signal from PpIX-containing liver-sample. The sample yielding the weaker signal (grey curve) contained less PpIX. The samples were kept in motion during the measurements. The integration time was 10 sec.

5.3 Focus-size investigation

The size of the focal point in fluorescence microscopy is of major importance; the smaller the focal-point, the better the spatial resolution. Since the two-photon excited signal is quadratically dependent on the intensity, the actual focus is theoretically smaller than for single-photon excitation. When calculating the focus-size for the current set-up, a cigar-shaped volume with a cross-section of 0.9 μm and a length of 7 μm was obtained, the borders at which the intensity had decreased by a factor of $1/e^2$. The corresponding volume for the single-photon case is approximately 1.3 μm cross-section times a length of 11 μm.

5.3.1 Imaging measurements

In order to measure the extension of the bleached region and hence estimate the volume of the focus, a sample of human serum stained with Photofrin was examined. Efforts were made to bleach a point and afterwards detect this as a dark spot in a bright image. The result is seen in *Fig 5.13*. The spot detected had elliptical form with a size of about 15*30 μm. This is much more than predicted by the theoretically calculated values. Three possible explanations of this unexpected result are:

- The volume bleached is much larger than the size of the focus volume.
- The focus in the present set-up is poorer than what was theoretically predicted.
- Diffusion in the serum due to heating of the sample and the un-smooth movement of the scanning stage makes the detected spot larger. The fact that the shape of the spot was oval make this explanation probable since the stage is scanning in mainly one dimension.

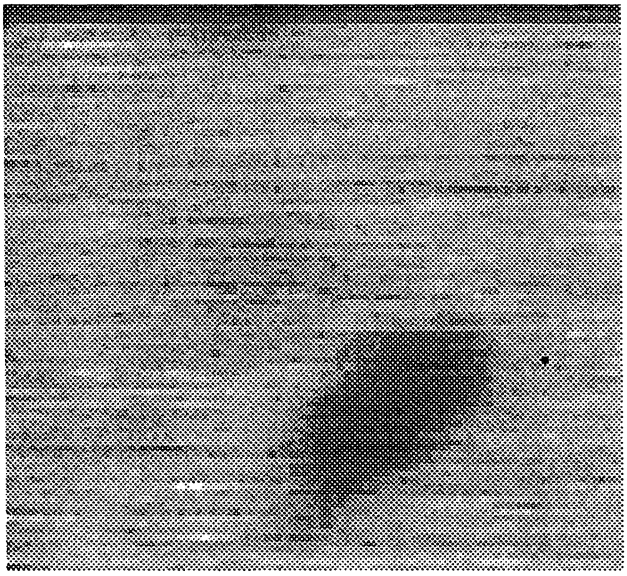

*Fig. 5.13. Image of human serum, 100*100 μm. The dark spot is due to bleaching. The size is approximately 15x30 μm.*

5.3.2 Spectroscopical measurements

To further investigate the size of the bleached volume, spectroscopic measurements were made at various distances from a bleached spot. The results from these experiments can be seen in *Figs. 5.14* and *5.15*.
The spectroscopic experiments indicate that the bleached spot is smaller than what the imaging experiments showed but still larger than the theoretical values. The spot seen in *Fig 5.13* is hence caused not only by bleaching of the Photofrin, but also probably enlarged by diffusion in the sample.
In the latter experiment, the limits of both the original spot and the measured spot were rather vaguely defined. No exact value for the focal-volume were therefore obtained, rather maximum values that the accurate measures are inferior to. The results

from the spectroscopic experiments show that the bleached volume has a cross-section-diameter of approximately 4 μm and a length of approximately 8 μm.
Fluorescence-signals from rat liver sample were recorded during 50 sec. (5*10 sec.). From the four spectra in *Fig. 5.14* it is seen that the spectra differ some in appearance, they are spectrally shifted after bleaching. This indicates that either the sample contains more than one fluorophore, or that the sample in-homogenous, yielding different fluorescence at different spots.

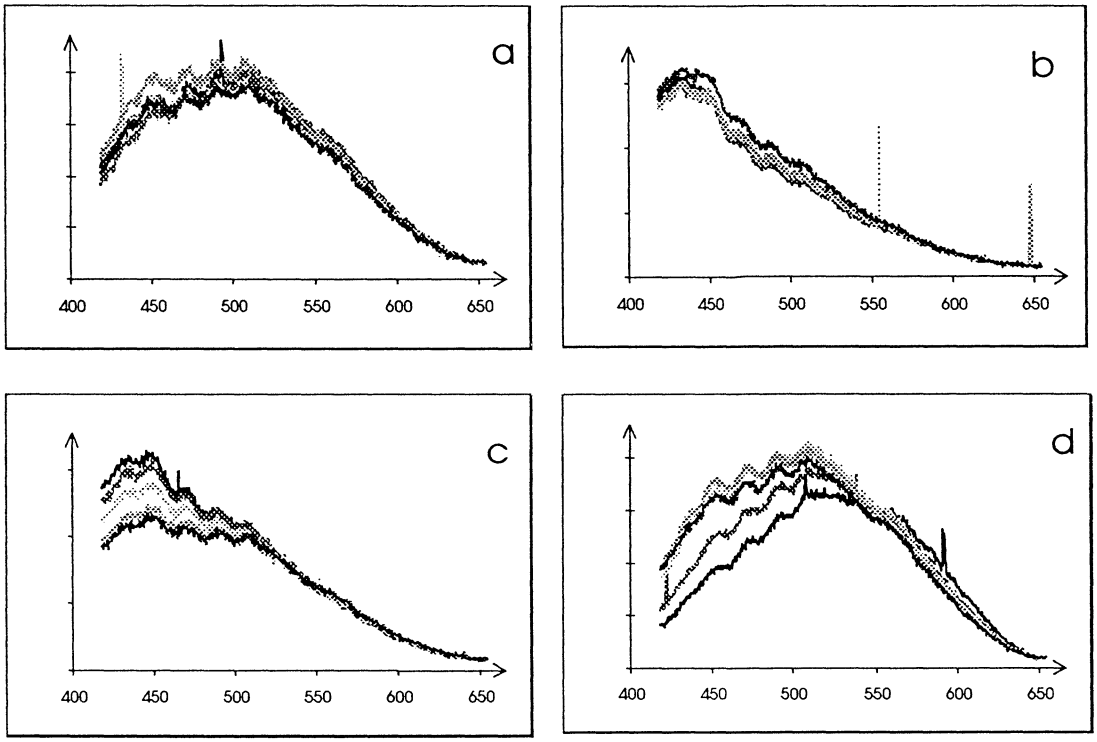

Fig. 5.14. Fluorescence signals from a rat-liver sample (intensity/a.u. as a function of wavelength/nm) at various horizontal distances from an illuminated (and thus bleached) spot:
(a) 0 μm (origo)
(b) 2 μm
(c) 3 μm
(d) 5 μm

The signal from the originally bleached spot, "origo", after a few minutes illumination, is shown in *Fig. 5.14a.* During the period of 50 seconds the signal level do not change much; the sample is already bleached the focal-point. The spectrum in *Fig. 5.14d* is detected 5 μm from origo and, as seen, this spot is bleached during the interval, which means that at this distance from origo no photobleaching takes place. *Fig. 5.14c* shows a spectrum detected 3 μm from the origo, this spot is moderately bleached. The spectrum in *Fig. 5.14b* is detected at 2 μm distance from origo, it is clearly seen that this spot is already bleached from the illumination of origo.
In *Fig. 5.15* fluorescence- signals from different vertical distances are shown. *Fig. 5.15a* shows a spectrum recorded at origo; no further bleaching. The spectrum in *Fig. 5.15b* is detected at 4 μm vertical distance from origo. Here, not much photobleaching takes place. In *Fig. 5.15c* though no bleaching has occurred before. This spectrum is from a distance of 5 μm from origo.

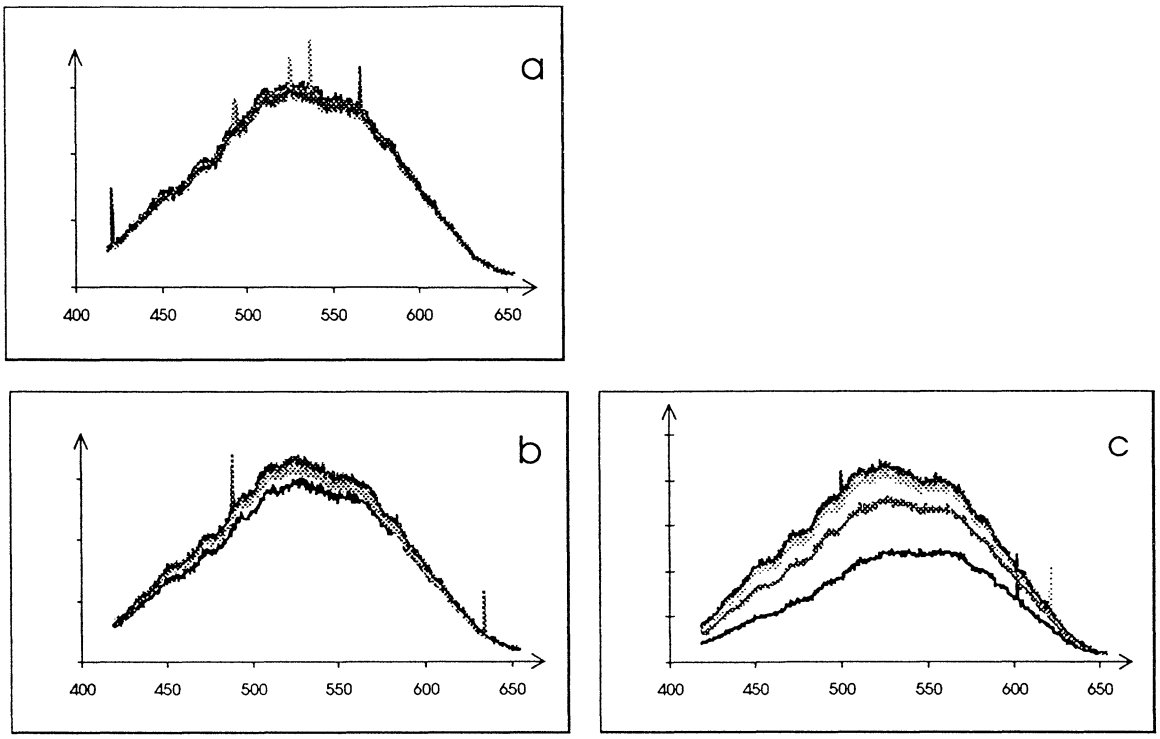

Fig. 5.15. Fluorescence signals from a rat-liver sample (intensity / a.u. as a function of wavelength / nm) at various vertical distances from an illuminated (and thus bleached) spot:
(a) 0 μm
(b) 4 μm
(c) 5 μm

6. Discussion and Conclusions

6.1 About the project

The original base for this diploma work was a bit vague. A variety of properties concerning two-photon excited fluorescence microscopy were to be investigated, and along the way even more questions have arisen. Setting the limits for this project has been a difficult task...
My effort has been concentrated on some major questions; such as optimising the imaging properties through finding the best suited optics for the two-photon excited technique and obliterating disturbances to make ALA-detection possible. The third major part has been to investigate the size of the excited volume. To estimate the volume bleached in focus and compare the results with theoretical calculations.
Both the first parts have given clear results, the optics are optimised and the pulse-broadening has been proved not to be significant. The disturbances hampering photosensitiser detection are eliminated, together with some other disturbing peaks. Consequently, it is now possible to clearly distinguish normal tissue from tissue containing photosensitiser; experiments showing this have been carried out.
The third part of the project was to experimentally study the size of the excited volume. The experimentally obtained size corresponded well with the theoretically calculated. The extension in the focal plane was, however, slightly larger than expected. Then again, the experimental results give only a rough idea of the focus-size and the experimentally obtained measures are to be seen as an outer limit of the real extension of the focal-point.

6.2 Future work

A drawback with the present experimental arrangement is that no spectral information about the fluorescence of the specimen can be obtained at wavelengths over ~700 nm. This is mainly because of the scattered-laser-light-induced background-signal that increases rapidly at about 700 nm. The dichroic mirror reflects wavelengths over 700 nm, some light around this wavelength is probably first reflected and then transmitted. To improve the detection of fluorescence above 700 nm, I suggest that the laser light is filtered through an interference filter, and that the BG39 Schott filter is changed to a hot-mirror with transmission up to 750 nm. [33] Then it would probably be possible to detect the PpIX-peak at 700 nm. In the present set-up this peak is efficiently suppressed by the background signal and can not be detected. An improved PpIX-detection technique could then be based on recognition of both the characteristic peaks.

In order not to have to blank the computer screen for every measurement, it would be preferable if the path between the exit of the microscope and the entrance of the spectrometer could be enclosed. The first step towards this is taken in this project but the second step remains: Designing a tube attachable to the periscope. This can be done as soon as the set-up is permanent. The spectrum quality would probably

improve even more than showed in this paper, since weak background light always finds its way into the lab and into the spectrometer in the present set-up.

Future investigations of the focus size may be made through the use of the equipment in *imaging mode*. A more interesting result than the ones here presented would probably be obtained if the viscosity of the sample examined was increased through use of another dissolvent, or if experiments were made on liver tissue. Optical sectioning of the focal point can be achieved if scans are made on different levels in the sample. Such measurements could shed some further light on the question about the size of the focal-point in two-photon fluorescence microscopy.

A comparison between single and two-photon exciting techniques concerning photobleaching and spectroscopic properties of porphyrins in tissue can be made. Corresponding experiments can be made using the present set-up and with a Krypton-laser as exciting light source for the single-photon excitation.

6.3 Conclusions

Through the use of two-photon excited fluorescence microscopy technique, high spatial and spectral resolution is obtained. It is also possible to distinguish normal tissue from tissue containing photosensitisers. These facts, together with existing technique and equipment, vouch for the possibility to develop a tool for investigation of the pharmacokinetics of various photosensitisers, and thus help to optimise the PDT outcome. The results obtained and the improvements made in this diploma project have hopefully given some valuable information for the future of the two-photon excited microscopy techniques, and for the development of the above mentioned tool.

7. Acknowledgements

First of all I would like to thank my tutor Ingrid Rokahr who has not only guided me through this project and answered my never ending stream of questions, but who also awoke my interest for medical physics in general.
Stefan Andersson-Engels has been of great help in many ways and an extensive source of knowledge.
I would also like to thank Lars Bengtsson at Bergström Instrument and the people at LRI instruments in Lund for temporary loans of equipment.

Appendix A: Terminology

PSF and OTF

The point spread function, PSF, is the normalised diffraction pattern formed by a point object. When the lens is perfect (diffraction-limited) the diffraction pattern consists of a bright central disc (the Airy disc) surrounded by a series of progressively fainter rings. If the lens is less than perfect the size of the central disc and the spacing of the surrounding rings stays about the same, but the central disc is less bright. The light that is lost from the central disc reappears in the surrounding rings.
The Fourier transform of the point spread function , $\Im\{\text{psf}\}$, describes how the spatial frequency components of the object are affected when imaged by the system. When normalised, the Fourier transform of the point spread function is called the transfer function or the Optical Transfer Function, OTF [35]:

$$\text{OTF}(\nu) = \frac{\Im\{\text{psf}\}}{\int_{-\infty}^{\infty} \text{psf}(x)dx} \qquad (A.1)$$

Numerical aperture (N.A.)

This value indicates the light acceptance angle of the objective (or any arbitrary optical system) and determines the light gathering power, the resolving power and the depth of focus. A numerical aperture can be defined for any optical system as N.A. = n $\sin\alpha$. It is dependent of the refractive index, n, of the immersion medium and on the angle α, defined in figure 9.1. If the numerical aperture is increased a better resolution is obtained, therefore a lens with a high N.A. is often preferred [20,29].

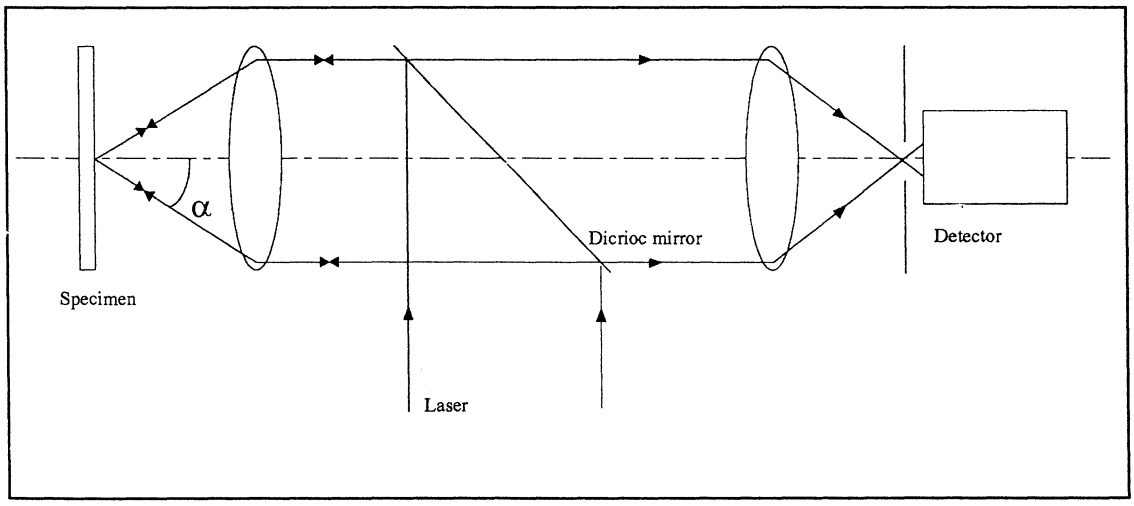

Fig. A.1. Definition of the numerical aperture: N.A. = n sin α.

Spatial frequencies and spatial frequency cut-off

Fourier analysis technique was originally applied in optics by people who were versed in linear circuit analysis. Unlike in electrical processing, where the signals vary in time, the information in optics is more often spread across a region of space at a specific moment. In circuit analysis the basic mathematical tool is the Laplace transform, while in optical analysis the more general Fourier transform is used. The Fourier transform $\hat{f}(v)$ of a function $f(x)$, where x is a spatial co-ordinate, is defined by

$$\hat{f}(v) = \int_{-\infty}^{+\infty} f(x) e^{-i2\pi vx} dx \qquad (A.2)$$

v is here called the spatial frequency and is defined in Eq. A.3. The spatial frequencies appear as linear co-ordinates in the focal plane of the lens on a scale determined by the wavelength of the light and the focal length of the lens:

$$v = \frac{x}{\lambda \cdot f} \qquad (A.3)$$

The dimension of the spatial frequency is length^{-1} and is given in cycles/ mm. [36,37]

The **spatial frequency cut-off** is accordingly the resolution limit of the imaging system; defining how fine patterns can be resolved. The larger the limit, the finer the patterns resolved.

Scanning stage / scanning beam

Scanning can be performed in two ways: either the specimen is moved and the laser beam is kept still or vice versa. The former method (the scanning stage method) is the simpler one and the one used in the present set-up. This method gives uniform imaging properties over the entire image; any off-axis aberrations are kept out. Precise high speed movement is however necessary and can be difficult to obtain.
Using beam scanning, no problems concerning movement of heavy objects are present, but off-axis aberration has to be considered. Accordingly the imaging properties may not be uniform over the entire image. *Fig A.2* shows the principle of a scanning beam technique [20].

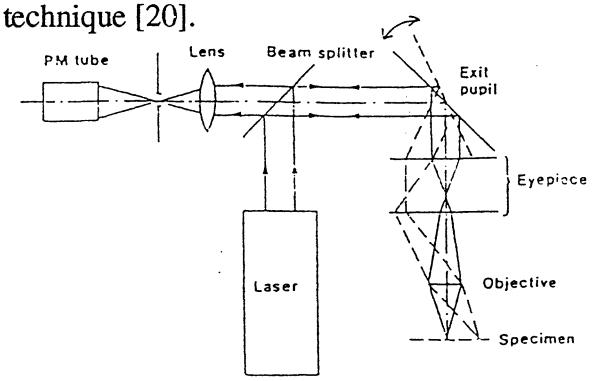

Fig A.2. Principle of a scanning beam microscope. [20]

Appendix B: Aberrations

Geometric optics is based on first-order theory; that **sin** α is approximated with α. This is a good approximation in the paraxial region, near the optical axis, but its results are inconsistent with exact ray-tracing outside this region. If the first two terms in the expansion

$$\sin\alpha = \alpha - \frac{\alpha^3}{3!} + \frac{\alpha^5}{5!} - \frac{\alpha^7}{7!} + \ldots \qquad (B.1)$$

are retained we have the so called third-order theory. The differences appeared are referred to as the five primary aberrations: **spherical aberration, coma, astigmatism, field curvature and distortion**. These five types of aberrations occur in all kinds of light imaging. Furthermore **chromatic aberration** which arise from the fact that the refractive index, n, is an aberration depending on the frequency of the light. Field curvature and chromatic aberration have been of most importance in this project. For a further description of aberrations I refer to Ref [37].

Field curvature. This phenomena implies that a plane perpendicular to the optical axis will be imaged as a paraboloidal surface. In *Fig. B.1,* a spherical object segment σ_0 is imaged by a lens as a spherical segment σ_i , both centred at O. The plane σ_o' ,will be imaged as a paraboloidal surface, Σ_p , (a *Petzval surface,* named after the Hungarian mathematician Josef Max Petzval). The Petzval surface curves towards the object plane for positive lens like in our case, and away from the object plane for a negative lens. Thus the field curvature can be compensated for by a combination of positive and negative lenses.

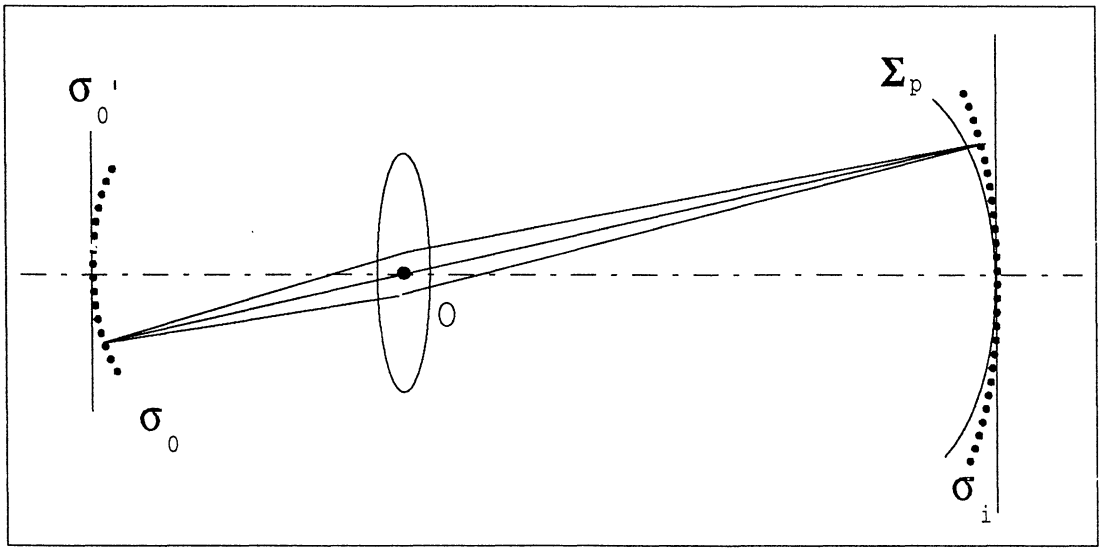

Fig. B.1. Field curvature.

Chromatic aberration. Rays of different colours will traverse an optical system along different paths. Since the thin-lens equation

$$\frac{1}{f}=(n-1)\left(\frac{1}{R_1}-\frac{1}{R_2}\right) \qquad (B.2)$$

is wavelength-dependent $(n=n(\lambda))$, the focal length of a certain lens also vary with the wavelength. The result of this fact is illustrated in *Fig. B.2.* The constituent colours in the incident beam are focused at different points along the optical axis.

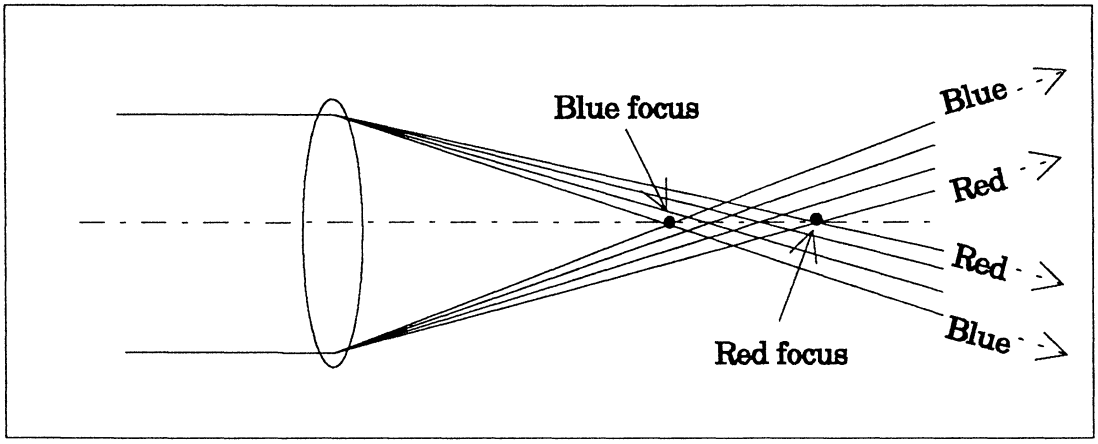

Fig. B.2. Chromatic aberration.

Chromatic aberration can be compensated for. While working in a specified wavelength region, the optical system can be designed to compensate for chromatic aberration in that specific region. [36,37]

Appendix C: Clinical tissue fluorescence measurements

To record fluorescence spectra from macroscopic tissue, another fluorosensor than the equipment described in chapter 4 is used. That system consists of a nitrogen-laser-pumped dye-laser, emitting light at 405 nm and an optical fiber to guide the excitation light to the sample and the fluorescence light back to a detector. The detector consists of a spectrometer connected to an air-cooled CCD-camera.
In *fig C.1* the spectrum recorded from a PpIX-containing rat-liver sample is shown.

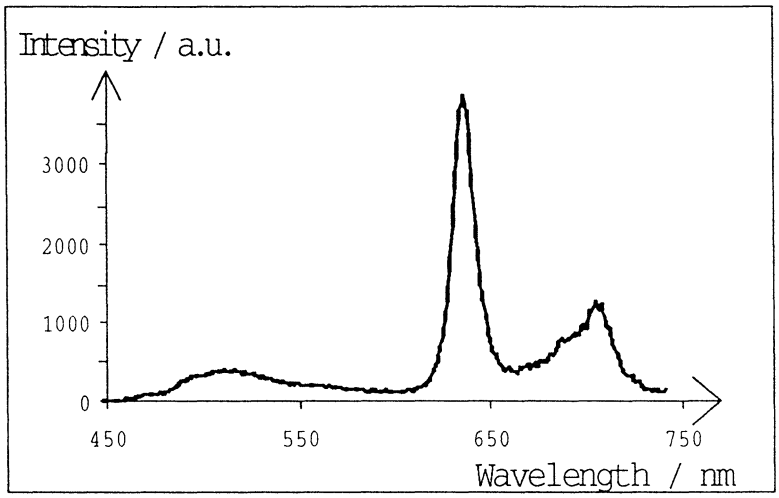

Fig. C.1. Spectrum from a rat liver containing ALA-induced proto-porphyrin IX.

References

1. K. Svanberg, ed., *Progress Report*, Lund University Medical Laser Centre, (1992).

2. C.-G. Wahlström, ed., *Progress Report 1993-1994,* (LRAP-172, Lund Institute of Technology, 1994).

3. S. Svanberg, *Atomic and Molecular Spectroscopy,* (Springer-Verlag, Berlin, 1992).

4. O. Trepte, I. Rokahr, S. Andersson-Engels and K. Carlsson, "Studies of porphyrin containing specimens using an optical spectrometer connected to a confocal scanning laser microscope," Journal of Microscopy **12,** vol 176, 238-244 (1994).

5. S. Andersson-Engels, *Laser-Induced Fluorescence for Medical Diagnostics,* (LRAP-108, Lund Institute of Technology, 1989).

6. A. Nilsson, "Diagnostik och behandling av cancer med hjälp av laser," Ung Forskning **1,** in press (1995).

7. V. Dominicand and J. Feinberg, "Light-Induced Second-Harmonic Generation in Glass via Multiphoton Ionization," Physical Review Letters **71**, 3446-3449 (1993).

8. E. M. Dianov and D. S. Starodubov, "Photoinduced Second-Harmonic Generation in Glasses and Glass Optical Fibers," Optical Fiber Technology **1**, 3-16 (1994).

9. M. Yoshida, Private Communication.

10. R. W. Boyd, *Nonlinear optics*, (Academic press inc., 1992).

11. C. J. R. Sheppard, R. Kompfner, J. Gannaway and D. Walsh, "The scanning harmonic optical microscope," IEEE Journal of Quantum Electronics, **QE-13** (1977).

12. C. J. R. Sheppard and R. Kompfner, " Resonant scanning optical microscope," Applied Optics **17**, 2879-2882 (1978).

13. W. Denk, J. H. Strickler and W. W. Webb, "Two-Photon Laser Scanning Fluorescence Microscopy," Science, **248,** 73-76 (1990).

14. W. Webb, "Two-photon excitation in laser scanning fluorescence microscopy," Trans. Roy. Microscopical Soc., Vol 1: Micro 90, H. Y. Eldner, ed., 445-450. Adam Hilger, Bristol (1990).

15. P. F. Curley. A. L. Ferguson, J. G. White and W. B. Amos, "Application of a femtosecond self-sustaining mode-locked Ti:sapphire laser in the field of laser scanning confocal microscopy," Opt. Quantum Electron. **24,** 851-859 (1992).

16. D. W. Piston, D. R. Sandison and W. W. Webb, "Time-resolved fluorescence imaging and background rejection by two-photon excitation laser scanning microscopy," SPIE **1640**, 379-389 (1992).

17. H. Szmacinski, I. Gryczynski and J. R. Lakowicz, "Calcium dependent fluorescence lifetimes of Indo-1 for one- and two-photon excitation of fluorescence," Photochem. Photobiol. **58**, 341-345 (1993).

18. M. Born and F. Wolf, *Principles of optics, 5th edition* (Pergamon press, Oxford 1975).

19. C. J. R. Sheppard and M. Gu, "Image formation in two-photon fluorescence microscopy," Optik **86,** 104-106 (1990); Erratum, *Optik* **92,** 102 (1992).

20. K. Carlsson, *Light Microscopy: an introduction to conventional and confocal microscopy,* (Physics IV, Rotal Institute of Technology, Stockholm, 1994).

21. A. J. Dixon, "Principles and applications of confocal fluorescence microscopy," EMAG-MICRO 89, 13-15 September, 643-650 (1989).

22. O. Nakamura, "Three-dimensional imaging characteristics of laser scan fluorescence microscopy: Two-photon excitation vs. single-photon excitation," Optik **93**, 39-42 (1993).

23. M. Gu and C. J. R. Sheppard, "Effects of a finite-sized pinhole on 3 D image formation in confocal two-photon fluorescence microscopy," Journal of Modern Optics, **40**, 2009-2024 (1993).

24. S. Andersson-Engels, I. Rokahr and J. Carlsson, "Time- and wavelength resolved spectroscopy in two-photon excited fluorescence microscopy," Journal of Microscopy **176,** 195-203 (1994).

25. F. W. D. Rost, *Fluorescence Microscopy,* vol 1, (Cambridge University Press, 1992).

26. G. J. Brakenhoff, K. Visscher and E. J. Gijsbers, "Fluorescence bleach rate imaging," Journal of Microscopy **175**, 154-161 (1994).

27. S. Svanberg, J. Larsson, A. Persson and C.-G. Wahlström, "Lund high-power laser facility-systems and first results," Physica Scripta **49**, 187-197 (1994).

28. I. Rokahr and S. Andersson-Engels, "Two-photon excited fluorescence microscopy combined with spectral and time-resolved measurements for fluorophore identification, "SPIE Photonics West '95", in press (1995).

29. *CF lenses,* (Nikon Corporation, Tokyo, 1989).

30. *FR-103 autocorrelator instruction manual,* Femtochrome research inc., (Berkeley CA., 1991).

31. U. Gustavsson, *Near-Infrared Raman Spectroscopy Using a Diod Laser and CCD Detector for Tissue Diagnostics*, (LRAP-138, Lund Institute of Technology, 1993).

32. A. Persson, Private communication (1995).

33. S. Hell and H. Hertz, Private communication, (1994).

34. *Optics Guide 5,* (Melles Griot 1990).

35. O. Franksson, *Imaging Systems*, (KTH, Stockholm, 1994).

36. S.-G. Pettersson, *Optisk Teknik/Advanced Optics,* (Lund, 1994).

37. E. Hecht, *Optics,* (Addison-Wesley Publishing Company, Reading, Massachusetts, 1987).